

**Chromosome painting and
arrangement of interphase chromosome territories
in *Arabidopsis thaliana***

Dissertation

zur Erlangung des akademischen Grades

doctor rerum naturalium (Dr.rer.nat.)

vorgelegt der

Mathematisch-Naturwissenschaftlich-Technischen Fakultät

(mathematisch-naturwissenschaftlicher Bereich)

der Martin-Luther-Universität Halle-Wittenberg

von Herrn Ales Pecinka

geb. am: 28.01.1978 in: Opava, Tschechische Republik

Gutachter:

1. Prof. Reuter
2. Prof. Schubert (Gatersleben)

Verteidigung: Halle (Saale), den 30.06.2005

urn:nbn:de:gbv:3-000008813

[<http://nbn-resolving.de/urn/resolver.pl?urn=nbn%3Ade%3Agbv%3A3-000008813>]

ACKNOWLEDGEMENTS

I would like to express my grateful thanks to my supervisor Prof. Dr. Ingo Schubert, the head of Cytogenetics Department, for giving me the opportunity to work in his group, for constant guidance, continuous support and encouragement.

I am very thankful to Dr. Armin Meister, Dr. Gregor Kreth, Prof. Dr. Eric Lam, Dr. Naohiro Kato, Dr. Koichi Watanabe, Dr. Martin A. Lysak, Dr. Célia Baroux, Dr. Andreas Houben, Dr. Jörg Fuchs, Dr. Veit Schubert, Dr. Aline V. Probst, Dr. Wim Soppe, Alexandre Berr, Dr. Sabina Klatte, Marco Klatte, Dr. Bernd Reiss and Dr. Jean Molinier, for their support and helpful discussions. Moreover, I would like to thank Martina Kühne, Achim Bruder, Rita Schubert, Ines Walde, Andrea Kuntze and Barbara Hildebrandt for their technical assistance.

Finally, I wish to express my gratitude to Conny, my parents, brother and friends, who have been a great support for me.

Content

1. INTRODUCTION	7
1.1. FLUORESCENCE IN SITU HYBRIDIZATION (FISH) FOR CHROMOSOME PAINTING ...	7
1.1.1. Principles and applications of FISH for chromosome painting	7
1.1.2. Feasibility of chromosome painting in plants.....	8
1.1.3. Aims of the work on chromosome painting in <i>A. thaliana</i>	9
1.2. INTERPHASE CHROMOSOMES: STRUCTURAL AND FUNCTIONAL ORGANIZATION	10
1.2.1. Arrangement of interphase chromosomes in various organisms.....	10
1.2.2. Aims of the work on interphase CT arrangement of <i>A. thaliana</i>	12
1.3. INFLUENCE OF TANDEM REPETITIVE TRANSGENES AND OF FLUORESCENT CHROMATIN TAGS ON THE INTERPHASE CHROMOSOME ARRANGEMENT	14
1.3.1. Lac operator/GFP-lac repressor chromatin tagging system.....	14
1.3.2. Aims of the work on inducible local alteration of interphase chromosome arrangement	15
2. MATERIALS AND METHODS	16
2.1. PLANT MATERIAL, PREPARATION OF CHROMOSOMES AND ISOLATION OF NUCLEI	16
2.2. DOT BLOT HYBRIDIZATION	17
2.3. PROBES	18
2.4. PROBE LABELING AND FISH	19
2.5. MICROSCOPIC ANALYSES	20
2.6. COMPUTER SIMULATIONS OF RANDOM CHROMOSOME ARRANGEMENT	21
2.6.1. Determination of dimensions and volumes of <i>Arabidopsis</i> nuclei.....	21
2.6.2. The 1 Mb Spherical chromatin domain model.....	22

2.6.3.	<i>Random spatial distribution model</i>	23
3.	RESULTS AND DISCUSSION	24
3.1.	ESTABLISHING OF CHROMOSOME PAINTING IN ARABIDOPSIS THALIANA	24
3.1.1.	<i>Development of painting probes for individual chromosomes</i>	24
3.1.2.	<i>Identification of misaligned BAC clones by FISH</i>	25
3.1.3.	<i>Identification of chromosome rearrangements by means of chromosome painting</i>	27
3.1.4.	<i>Conclusions as to the chromosome painting in Arabidopsis thaliana</i>	29
3.2.	ARRANGEMENT OF INTERPHASE CTs AND SOMATIC HOMOLOGOUS PAIRING IN NUCLEI OF A. THALIANA	31
3.2.1.	<i>The relative positioning of entire CTs is random</i>	31
3.2.2.	<i>The association frequency of homologous chromosome arm territories is random for chromosomes 1, 3, 5 and higher for chromosomes 2 and 4</i> .	33
3.2.3.	<i>The relative position of a gene (FWA) within its CT does not necessarily reflect the transcriptional state</i>	36
3.2.4.	<i>Somatic pairing of homologous chromosome segments occurs at random</i>	38
3.2.5.	<i>The frequency of somatic homologous pairing is not altered in Arabidopsis mutants with an increased frequency of somatic homologous recombination</i>	42
3.2.6.	<i>Conclusions as to the arrangement of interphase CTs and somatic homologous pairing</i>	44
3.3.	ALTERATION OF THE LOCAL INTERPHASE CHROMOSOME ARRANGEMENT BY TANDEM REPETITIVE TRANGENES AND FLUORESCENT CHROMATIN TAGS	46

3.3.1.	<i>GFP spot numbers vary in 2C live nuclei of homozygous transgenic plants (EL702C) harboring two tagged loci on the top arm of chromosome 3.....</i>	46
3.3.2.	<i>GFP spots always co-localize with FISH signals of lac operator arrays, but not vice versa</i>	48
3.3.3.	<i>Lac operator arrays pair more often than random in nuclei of transgenic plants and thus enhance pairing frequency of adjacent endogenous regions.....</i>	49
3.3.4.	<i>The transgenic tandem repeats co-localize more often than the flanking regions with heterochromatic chromocenters.....</i>	54
3.3.5.	<i>Conclusions as to the local alterations of interphase chromosome arrangement caused by repetitive transgenes and fluorescent chromatin tags.....</i>	57
4.	OUTLOOK.....	58
5.	SUMMARY	60
6.	ZUSAMMENFASSUNG	63
7.	LITERATURE.....	66
	PUBLICATIONS IN CONNECTION WITH THE SUBMITTED DISSERTATION	75
	DECLARATION ABOUT THE PERSONAL CONTRIBUTION TO THE MANUSCRIPTS FORMING THE BASIS OF THE DISSERTATION	76
	EIDESSTATTLICHE ERKLÄRUNG	77
	CURRICULUM VITAE.....	78
	APPENDIX	79

List of abbreviations

3D	3-dimensional	dUTP	2'-deoxyuridine 5'-triphosphate
BAC	bacterial artificial chromosome	FISH	fluorescence <i>in situ</i> hybridization
C	1C corresponds to the DNA content of unreplicated reduced chromosome complement	GFP	green fluorescence protein
Col	Columbia	GISH	genomic <i>in situ</i> hybridization
CP	chromosome painting	<i>Ler</i>	Landsberg <i>erecta</i>
CT	chromosome territory	NLS	nuclear localization signal
DAPI	4',6-Diamidino-2-phenylindole	NOR	nucleolar organizer region
dATP	2'-deoxyadenosine 5'-triphosphate	rDNA	ribosomal DNA
dCTP	2'-deoxycytidine 5'-triphosphate	RSD	random spatial distribution
DEAC	diethyl aminomethyl coumarin	SCD	spherical chromatin domain
Dex	Dexamethasone	SDS	sodium dodecyl sulphate
dGTP	2'-deoxyguanosine 5'-triphosphate	Tris	Tris-(hydroxymethyl)-aminomethan
DNP	2,4-dinitrophenyl	UV	ultraviolet
dTTP	2'-deoxythymidine 5'-triphosphate	WS	Wassilewskija
		WT	wild-type

1. Introduction

The thesis is divided into three main parts. The first one has predominantly methodological character and describes the development of chromosome specific probes for chromosome painting in the model plant *Arabidopsis thaliana*. In the second part, arrangement of chromosome territories (CTs) in *Arabidopsis* nuclei of different ploidy and from various organs is characterized and compared to the predictions derived from computer model simulations of a presumed random arrangement. In the third part, the influence of a transgenic tandem repeat with a fluorescent tag (lac operator/GFP-lac repressor-NLS) on the local interphase chromosome arrangement is elucidated.

1.1. Fluorescence in situ hybridization (FISH) for chromosome painting

1.1.1. Principles and applications of FISH for chromosome painting

Fluorescence *in situ* hybridization (FISH) is a method for microscopic detection of specific sequences in a genome, utilizing nucleic acid probes with complementarity to the target sequences. The term chromosome painting (CP) was introduced by Pinkel et al. (1988) for *in situ* visualization of specific chromosomes or large chromosome segments within chromosome complements by FISH. For vertebrates, specific painting probes have been amplified by degenerate oligonucleotide primed-polymerase chain reaction from either flow-sorted or microdissected chromosomes (reviewed in Langer et al. 2004). To achieve chromosome specific signals, labeled repeats of the painting probe with a dispersion extending to other than the target regions have to be prevented from

hybridization by excess of unlabelled genomic DNA. Therefore, this technique was denominated also ‘chromosomal in situ suppression’ hybridization (Lichter et al. 1988).

Recently, a broad spectrum of CP techniques suited for different applications in research and clinical diagnostics has been developed (reviewed in Ferguson-Smith 1997; Ried et al. 1998; Langer et al. 2004). CP became a powerful tool for identification of chromosomes and chromosome rearrangements (e.g. Lichter et al. 1988; Blenow 2004), for mutagenicity testing (e.g. Cremer et al. 1990; Marshall and Obe 1998; Natarajan et al. 1992) and for studies of chromosome organization and dynamics during interphase (reviewed in Cremer and Cremer 2001; Parada and Misteli 2002; Bickmore and Chubb 2003) as well as for studies of chromosome/karyotype evolution (e.g. Wienberg and Stanyon 1995; Svartman et al. 2004).

1.1.2. Feasibility of chromosome painting in plants

Although CP underwent dramatic progress in animal and human cytogenetics during the last decade, attempts to establish CP in euploid plants have failed. This is probably due to the large amounts of complex dispersed repeats that are more or less homogeneously distributed over all chromosomes (reviewed in Schubert et al. 2001). Specific painting of plant chromosomes could be achieved only by genomic *in situ* hybridization (GISH), within genomes of interspecific hybrids or their progenies, using genomic DNA of one parental species as a probe (Schwarzacher et al. 1989). On the basis of chromosome-specific repeats, B (Houben et al. 1996) and sex chromosomes (Shibata et al. 1999; Hobza et al. 2004) could be painted with chromosome derived probes.

The situation has changed since *Arabidopsis* with its small genome (~157Mb/1C), low amount of repetitive DNA sequences, clustered mainly in the

(peri)centromeric regions and nucleolus organizer regions (NORs) (The Arabidopsis Genome Initiative 2000; Bennett et al. 2003) became suitable for CP due to the public availability of bacterial artificial chromosome (BAC) contigs covering the entire chromosome complement (Scholl et al. 2000). The breakthrough was accomplished by taking advantage of high-resolution FISH on pachytene chromosomes (Fransz et al. 1998, 2000) and the application of BAC contig pools as probes according to a method previously applied to paint yeast chromosomes (Scherthan et al. 1992). Arabidopsis chromosome 4 became the first entirely painted chromosome of a euploid plant karyotype (Lysak et al. 2001). A FISH approach based on the use of large insert clones (BACs/YACs) was at least partially successful to label a specific target region also for other plants with small genomes and relatively low content of repetitive sequences, e.g. sorghum, rice, cotton, tomato, potato and *Medicago* (reviewed in Lysak et al. 2001).

1.1.3. Aims of the work on chromosome painting in *A. thaliana*

After development of painting probes for the arms of Arabidopsis chromosome 4 (Lysak et al. 2001) it was aimed to develop chromosome-specific probes for all chromosomes of *A. thaliana* for a spectrum of possible applications, such as:

- discrimination of individual chromosomes and their rearrangements during all developmental and cell cycle stages.
- investigation of potential dynamics of CT arrangement during developmental and cell cycle stages.
- investigation of interphase chromosome arrangement and karyotype evolution in related *Brassicaceae* species.

1.2. Interphase chromosomes: structural and functional organization

1.2.1. Arrangement of interphase chromosomes in various organisms

Conventional microscopic studies on interphase nuclei reveal chromatin regions of different density/staining intensity, representing (positively heteropycnotic) heterochromatin fractions of high density (Heitz 1928), euchromatin of lower density and nucleoli of lowest density. A territorial organization of interphase chromosomes was first proposed by Rabl (1885). Complete interphase CTs could be traced only one century later when CP by FISH became established and allowed to determine the arrangement of CTs within nuclei by 3-dimensional (3D) microscopy (Cremer and Cremer 2001).

Two models considering different aspects of nuclear CT distribution have been proposed (Parada and Misteli 2002). One model, based on the radial arrangement of CTs between the center and the envelope of the nucleus, suggests that gene-dense chromosomes are located more internally than gene-poor ones. Such an arrangement was found in various types of mammalian and chicken cells (Cremer et al. 2001; Habermann et al. 2001; Kozubek et al. 2002) and appeared to be evolutionarily conserved when the positions of homeologous chromosomes were compared between human and higher primates (Tanabe et al. 2002) or human and mouse (Mahy et al. 2002a). However, no such arrangement was found in non-cycling cells by Bridger et al. (2000). The other model reflects specific neighborhood relationships between two or more CTs or distinct chromosome domains. Non-random side-by-side arrangement of interphase CTs is of special interest because spatial vicinity of homologues is required, at least transiently and/or position-specific, for DNA repair via homologous

recombination between homologues, often yielding reciprocal translocations (Rieger et al. 1973; Parada and Misteli 2002), and transvection; i.e. homologous pairing influencing the gene activity (most of the cases are described in *Drosophila*, however, examples from plants, fungi and mammals are also known; reviewed in Duncan 2002). At least transient pairing is believed to play a role in establishment of paramutation; i.e. *trans* interactions between homologous sequences which set up distinct epigenetic states that are heritable (Chandler and Stam 2004; Stam and Mittelsten Scheid *in press*). In human cells non-random association of homologues is apparently restricted to certain chromosomes of distinct cell types, e.g. Sertoli cells (Chandley et al. 1996; Nagele et al. 1999). The relative positioning of all human heterologue combinations was proposed to be predominantly random (Cornforth et al. 2002). At least transient somatic association of homologous chromosomes has been claimed for yeast (Burgess et al. 1999), however, no clear evidence for such an association was found by others (Fuchs et al. 2002; Lorenz et al. 2003). A development- and cell cycle-specific close spatial alignment of homologous chromosome segments in nuclei of most somatic tissues was hitherto observed only in *Drosophila* (Hiraoka et al. 1993; Csink and Henikoff 1998; Fung et al. 1998). For review of somatic homologous pairing see McKee (2004). Recent studies have shown by photobleaching of fluorescently labeled chromatin *in vivo* that the positioning of interphase chromosomes is largely inherited from mother to daughter nuclei in mammals (Gerlich et al. 2003; Walter et al. 2003; see also Bickmore and Chubb 2003; Parada et al. 2003; Williams and Fisher 2003).

In plants with large genomes (>5,000 Mb/1C) interphase chromosomes frequently show Rabl orientation with centromeres and telomeres clustered at opposite poles of a nucleus (Dong and Jiang 1998) thus maintaining telophase arrangement. In *Arabidopsis* nuclei, instead of Rabl orientation, centromeres are randomly distributed in peripheral positions, while telomeres are clustered around the nucleolus (Fransz et al.

2002). Until recently, individual CTs could be traced in plant interphase nuclei only for single alien chromosomes within the chromosome complements of backcross progenies from interspecific hybrids by GISH (Schwarzacher et al. 1989). In case of disomic additions, close spatial association of the added homologues barely occurs in somatic nuclei (Schwarzacher et al. 1992; Abranches et al. 1998; Schubert et al. 1998; Martinez-Perez et al. 2001) except for tapetum cells of wheat (Aragon-Alcaide et al. 1997). However, it remains unclear whether the alien chromosomes behave in the same way as in their native background or as the host chromosomes. FISH experiments in diploid rice indicated homologous association of centromeres and telomeres but not of interstitial regions in root xylem and undifferentiated anther cells (Prieto et al. 2004). A significant and chromosome-specific degree of association of homologous centromeres was found in *Arabidopsis* nuclei (Fransz et al. 2002), but it remained open to what degree entire chromosome arms are involved. To answer these questions, our group has established recently chromosome specific painting of entire chromosomes of *Arabidopsis* and its close relatives using *A. thaliana* painting probes (Lysak et al. 2001, 2003; Pecinka et al. 2004).

1.2.2. Aims of the work on interphase CT arrangement of *A. thaliana*

Great progress has been achieved from studies of CT arrangement in vertebrate nuclei during the last decade. An increasing evidence for non-random radial and (at least sometimes also) side-by-side arrangement of CTs has been provided. In contrast to that, the organization of plant interphase chromosomes remained largely unknown. Using chromosome specific painting probes for *Arabidopsis* chromosomes, it was aimed to unravel CT arrangement in this plant and to answer the following questions:

- do Arabidopsis interphase CTs show a specific side-by-side or radial arrangement?
- does the CT arrangement differ between nuclei of different ploidy and from various organs?
- does the gene activity determine its position within a CT?
- to what extent does somatic homologous pairing occur in Arabidopsis?
- do Arabidopsis lines with an altered homologous recombination frequency in somatic tissues reveal a deviating frequency of somatic homologous pairing?

1.3. Influence of tandem repetitive transgenes and of fluorescent chromatin tags on the interphase chromosome arrangement

1.3.1. *Lac* operator/GFP-lac repressor chromatin tagging system

In situ localization and direct *in vivo* visualization of distinct chromosome regions recently became feasible by chromatin tagging systems. The *lac* operator/lac repressor system (Robinett et al. 1996; Straight et al. 1996) for instance uses a bacterial DNA binding protein (lac repressor) that, when fused with a green fluorescent protein (GFP) and a nuclear localization signal (NLS) peptide, binds to the 256 copies of directly repeated *lac* operators (~10 kb) integrated at a specific chromosome locus. Binding at the target locus yields a fluorescent spot of higher intensity than the overall fluorescence of dispersed unbound GFP molecules in the nucleoplasm. The GFP-lac repressor protein is either transiently or stably expressed. The system was applied to various eukaryotes such as yeasts (Aragon-Alcaide and Strunnikov 2000; Fuchs et al. 2002; Nabeshima et al. 1998; Straight et al. 1996), flies (Gunawardena and Rakowski 2000, Vazquez et al. 2002), cultured mammalian cells (Robinett et al. 1996; Tsukamoto et al. 2000), and plants (Kato and Lam 2001; Esch et al. 2003; Matzke et al. 2003). It revealed structural dynamics of chromosomes in interphase as well as mitotic nuclei by tracing the tagged loci in living cells (reviewed in Belmont et al. 1999; Gasser 2002; Lam et al. 2004).

However, such tagging systems generate artificial chromosome loci and unusual nuclear protein localization. For instance, in baby hamster kidney cells in which a *lac* operator array is amplified about 10 times, a nuclear protein complex, the so-called promyelocytic leukaemia body, is formed at the integration locus (Tsukamoto et al. 2000). Promyelocytic leukaemia bodies are thought to play a role in regulating

transcription. Because these bodies are not formed at the transgene locus without accumulation of the *lac* operator binding fusion protein, they are thought to recognize high concentrations of foreign proteins (Tsukamoto et al. 2000).

1.3.2. Aims of the work on inducible local alteration of interphase chromosome arrangement

Previously, the *lac* operator/lac repressor system was used to compare chromosome dynamics in *Arabidopsis* nuclei of different ploidy (Kato and Lam 2003), e.g. in 2C nuclei of guard cells (stomata) and in nuclei of pavement cells (8C on average). Frequently, a lower-than-expected number of GFP spots (two for hemizygous and four for homozygous EL702C plants) was observed (Kato and Lam 2003). Interestingly, Esch et al. (2003) also reported reduced number of GFP spots (only one spot per homozygous *lac* operator locus) in almost all nuclei of another *lac* operator/lac repressor tagged *Arabidopsis* line. These data suggested frequent alignment of allelic sequences, which was, however, not found for endogenous loci in *Arabidopsis* nuclei by Pecinka et al. (2004). Therefore it was aimed to test, whether the reduced number of GFP spots are indeed due to associations of operator arrays in *Arabidopsis* nuclei. In particular, it should be clarified what is the impact of the *lac* operator arrays and/or of the expression of the GFP-lac repressor protein on allelic/ectopic homologous pairing of *lac* operator arrays in comparison to average euchromatic regions.

2. Materials and methods

2.1. *Plant material, preparation of chromosomes and isolation of nuclei*

The following *A. thaliana* genotypes were used for preparation of pachytene chromosomes: Columbia (Col), Wassilewskia (WS), C24 (see Lysak et al. 2003; Pecinka et al. 2004), homozygous EL702C (Kato and Lam 2003; Pecinka et al. J. Cell Sci, *submitted*) and T665-IST (Aufsatz et al. 2002). Interphase chromosome arrangement and somatic homologous pairing were studied using the genotypes Col, Landsberg *erecta* (*Ler*) and the mutant *fwa-1* in *Ler* background (Soppe et al. 2000; Pecinka et al. 2004), C24 and the mutant *Atp150caf-1* in C24 background (Kyryk et al. manuscript in prep.), the mutants B71, P24I8, W92 and the control line IC9 (Molinier et al. 2004; J. Molinier and B. Hohn unpublished data). The influence of tandem repetitive transgenes on the arrangement of interphase chromosomes was studied in hemizygous and homozygous EL702C genotypes in Col background (Kato and Lam 2003; Pecinka et al. J. Cell Sci, *submitted*). Plants were cultivated as described in the referred papers.

Pachytene chromosomes were prepared according to Lysak et al. (2001). Inflorescences were fixed in ethanol/acetic acid (3 : 1) at least for 48 hours, rinsed in distilled water (2 x 5 min) and in citric buffer (10 mM sodium citrate, pH 4.8; 2 x 5 min) and incubated in 0.3% (w/v) pectolyase, cellulase and cytohelicase (Sigma, Germany) in citric buffer at 37°C for 2-3 h. Then the material was transferred into citric buffer and kept at 4°C. Individual flower buds were detached and macerated in 30 μ l of 50% acetic acid on microscopic slides. The slides were placed on a hot plate (45°C) and the drop was gently stirred by a needle for 30-60 seconds. Subsequently, 200 μ l of ethanol/acetic acid (3 : 1) were added and then the slide was dried by a hair drier. The

preparations were post-fixed in 4% formaldehyde in distilled water (v/v) for 10 min, air-dried and stored at 4°C until use.

For isolation of interphase nuclei, young root tips and rosette leaves were fixed for 20 min in 4% formaldehyde in Tris buffer (100 mM Tris-HCl pH 7, 5 mM MgCl₂, 85 mM NaCl, 0.1% Triton X 100) and homogenized in Tris buffer. Suspended nuclei were stained with DAPI (1 μg/ml) and flow-sorted according to their ploidy level using a FACStar^{Plus} flow cytometer (Becton Dickinson) equipped with an Argon-ion laser (INNOVA 90C-5) emitting UV light. Per ploidy level ~1000 nuclei were sorted onto microscopic slides in a drop of buffer containing 100 mM Tris, 50 mM KCl, 2 mM MgCl₂, 0.05% Tween and 5% of sucrose, air-dried and used for FISH or stored at –20°C until use. The nuclei of Arabidopsis lines carrying *lac* operator/*lac* repressor transgenes were prepared with the following modifications. To induce expression of the GFP-*lac* repressor-NLS protein, young rosette leaves were detached from the plants and floated in 10 ml of 0.3 μM (homozygous EL702C) or 3 μM (wild-type) Dexamethasone (Dex) solution in water in Petri dishes for 6-12 h. To avoid loss of GFP signals, leaves were fixed in 4% formaldehyde freshly prepared from paraformaldehyde and the 2C nuclei were sorted as described above.

2.2. Dot Blot hybridization

BAC clones purchased from the Arabidopsis Biological Resource Center (ABRC, Columbus, OH) were tested for the presence of high copy sequences by radioactive DNA-DNA dot blot hybridization. Approximately 0.4 μg of DNA per BAC clone was applied to the Minifold 1 Dot Blot system (Schleicher and Schnell) and fixed on moistened (2 x SSC) nitrocellulose N+ membrane (Hybond) under vacuum. The DNA was

denatured by adding 200 µl of 0.4 M NaOH per slot. Membranes were rinsed in 2 x SSC for 1 min and directly used for hybridization or stored at 4°C until use.

Genomic DNA from *A. thaliana* Col was isolated using a DNeasy Plant Mini Kit (Quiagen). Isolated DNA was sonicated to a fragment size of 100-500 bp and radioactively labelled with [α -³²P]-dCTP using a HexaLabel DNA Labeling Kit (Fermentas).

For Dot Blot hybridization, membranes were placed into a hybridization bottle with 5 ml of pre-hybridization solution [5 x SSPE (0.9 M NaCl, 0.05 M Sodium phosphate, 0.005 EDTA pH 7.7), 5 x Denhard's solution, 0.5% SDS] and 500 µl (10 µg/µl) of denatured (at 100°C for 5 min) salmon sperm DNA and incubated at 65°C for 5 h. Then, the radioactively labelled genomic DNA was added for at least 12 h at 65°C. The membranes were washed (in 0.5% SDS/2 x SSC; in 0.5% SDS/0.5 x SSC and in 0.5% SDS/0.1 x SSC; 20 min each at 65°C), wrapped in a plastic foil and screened with a Phosphoimager STORM860 using the ImageQuant software (Molecular Dynamics).

2.3. Probes

All BACs were obtained from the Arabidopsis Biological Resource Center (Columbus, OH). DNA of individual clones was isolated by standard alkaline extraction (Sambrook and Russell 2001). Clones that according to sequence annotation of The Institute for Genomic Research (Rockville, MD; <http://www.tigr.org/>) database harbour >5% of mobile elements and/or yielded strong signals (see Figure 3A) in Dot Blot hybridization (Lysak et al. 2003) were omitted from probes designed for CP (the list of BACs selected for CP of all Arabidopsis chromosomes is provided as Appendix).

Somatic homologous pairing was tested using the following BACs (Figure 7C): F6F3, F22L4, T2P11, T7N9, F11P17, T1F9, T11I11, F3F9 (all from chromosome 1,

GenBank accession Nos. AC023628, AC061957, AC005508, AC000348, AC002294, AC004255, AC012680, AC013430, respectively), F18C1, MGL6 (both from chromosome 3, accession Nos. AC011620 and AB022217), F4C21, F9H3, F13C5, T18B16, F6I7, F24A6, M7J2, F17I5 and F10M10 (all from chromosome 4, accession Nos. AC005275, AF071527, AL021711, AL021687, AL049657, AL035396, AL022197, AL031032, AL035521, respectively).

For the experiments with lac operator/lac repressor-NLS tagged lines, the following DNA clones were used in addition to BACs MGL6 and F18C1 (GenBank accession Nos. AB022217 and AC011620, respectively): BAC T15P10 containing 45S rDNA (accession No. AF167571), the plasmid 128x lacO-SK (Kato and Lam 2001), the plasmid pAL1 containing the 180 bp centromeric tandem repeat of *A. thaliana* (Martinez-Zapater et al. 1986) and a BAC contig spanning 4.2 Mb of chromosome 3 top arm from F2O10 to MSL1 (accession Nos. AC013454 and AB012247, respectively).

2.4. Probe labeling and FISH

BAC DNA was labeled by nick translation, either individually or, for CP, in pools of 4-5 BACs (19-38 such pools per chromosome). Labeled nucleotides (either biotin-dUTP, digoxigenin-dUTP, DNP-dUTP, Cy3-dUTP or DEAC-dUTP) were prepared as described by Henegariu et al. (2000). The quality of each labeled probe was tested individually on pachytene chromosomes.

Prior to FISH, slides were rinsed in 2×SSC (2 x 5 min), treated with pepsin (100 µg/ml in 0.01 M HCl) for 3-10 min at 38°C, rinsed in 2×SSC (2 x 5 min), post-fixed in 4% formaldehyde/2×SSC (10 min), rinsed in 2×SSC (2 × 5 min), dehydrated in 70, 90, 96% ethanol (2 min each) and air-dried.

For CP, the entire labeled probe (~110 ng of DNA of each BAC) was precipitated and resuspended in 20-40 μ l of hybridization mix (50% formamide, 10% dextran sulphate, 2xSSC, 50 mM sodium phosphate pH 7.0) per slide. After mounting the probe, the slides were placed on a heat block at 80°C for 2 min and then incubated in a moist chamber at 37°C for ~12-36 h.

Post hybridization washes and detection steps were as described (Schubert et al. 2001). Biotin-dUTP was detected by avidin conjugated with Texas Red (1:1000; Vector Laboratories), goat-anti-avidin conjugated with biotin (1:200; Vector Laboratories) and again with avidin conjugated with Texas Red, digoxigenin-dUTP by mouse-anti-digoxigenin (1:250; Roche) and goat-anti-mouse conjugated with Alexa-488 (1:200; Molecular Probes), DNP-dUTP by rabbit-anti-DNP (1:400; Sigma) and goat anti-rabbit conjugated with Cy5 (1:100; Jackson Laboratories). Cy3-dUTP and DEAC-dUTP were observed directly. Nuclei and chromosomes were counterstained with 1-2 μ g/ml of DAPI in Vectashield mounting medium (Vector Laboratories).

2.5. Microscopic analyses

Analysis of fluorescence signals was performed with an epifluorescence microscope (Axioplan 2; Carl Zeiss) using a 100x/1.4 Zeiss plan-apochromat objective and a cooled CCD camera Spot 2e (Diagnostic Instruments). Images were captured separately for each fluorochrome using appropriate excitation and emission filters. Single plane images and stacks of optical sections through nuclei were acquired with MetaVue software (Universal Imaging). The deconvolution of image stacks was performed with the 'point spread function' algorithm. Monochromatic images were pseudocoloured and merged using MetaMorph (Universal Imaging) and/or Adobe Photoshop 6.0 (Adobe Systems) software.

2.6. Computer simulations of random chromosome arrangement

2.6.1. Determination of dimensions and volumes of Arabidopsis nuclei

At first, the average volumes of 2C (*root*=25.9 μm^3 ; *leaf*=26.7 μm^3) and 4C (*root*=44.9 μm^3 ; *leaf*=39.9 μm^3) nuclei ($n>30$) were determined on the basis of 3D image stacks for nuclei of the three predominant shapes (flattened sphere, spindle and rod, Figure 1, Table 1). (Measurements were performed together with V. Schubert)

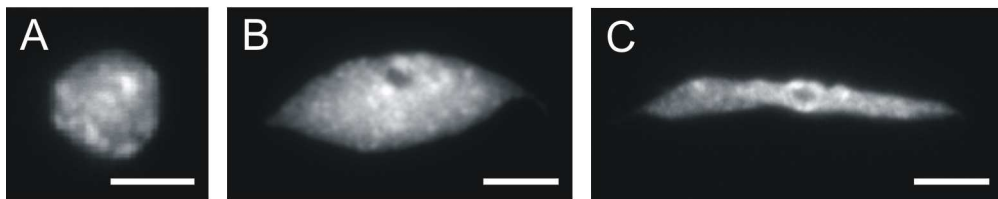


Figure 1. The three predominant shapes of Arabidopsis nuclei. (A) Flattened sphere, (B) spindle and (C) rod. Nuclei were counterstained with DAPI. Bars, 3 μm .

Table 1 Dimensions and volumes of different types of nuclei used for computer model simulations (Per organ and ploidy level the mean values were used.)

Organ	Ploidy	Nuclear shape	n	Axis length (μm)			Volume (μm^3)
				x	y	z	
root	2C	sphere	30	5.2	4.1	1.9	22.4
		spindle	30	9.4	3.2	1.9	30.0
		rod	31	14.3	1.8	1.8	25.4
	4C	sphere	32	6.6	5.3	2.2	43.5
		spindle	31	10.2	3.6	2.2	43.8
		rod	31	18.8	2.4	2.1	47.5
leaf	2C	sphere	32	5.1	4.4	2.1	25.7
		spindle	32	7.1	3.7	2.0	27.9
		rod	32	10.3	2.5	2.0	26.4
	4C	sphere	32	6.1	5.2	2.0	34.4
		spindle	32	8.7	4.4	2.2	43.4
		rod	32	12.7	3.0	2.1	41.3

2.6.2. The 1 Mb Spherical chromatin domain model

To assess the 3D topology of CTs within *Arabidopsis* nuclei, experimental data were compared with the prediction derived from computed simulations of random association of CTs according to the ‘spherical 1 Mb chromatin domain’ (SCD) model (Cremer et al. 2001; Kreth et al. 2004). Based on the compartmentation of interphase CTs into subchromosomal replication foci of 400-800 nm in diameter (Zink et al. 1998), the SCD model considers CTs as a chain of domains of ~1 Mb (500 nm in diameter) connected by entropic spring potentials. According to their DNA content (The *Arabidopsis* Genome Initiative 2000) chromosomes 1 to 5 should correspond 29, 20, 23, 18 and 26 Mb domains, respectively. To permit only minor overlaps, a repulsive potential between the domains was modeled and a weak energy barrier, essential for maintenance of a territorial organization of simulated chromosomes, was applied around each CT. As a start configuration, the model assumes compressed cylinders corresponding to the mitotic state of the chromatin domains of the 10 chromosomes to be statistically distributed within a simulated nucleus. The ‘start cylinders’ are then allowed to relax according to the ‘Metropolis Importance Sampling Monte Carlo’ method until the thermodynamic equilibrium is reached (Figure 2). Relaxed CTs fill the nucleus uniformly after ~200,000 Monte Carlo cycles (Metropolis et al. 1953).

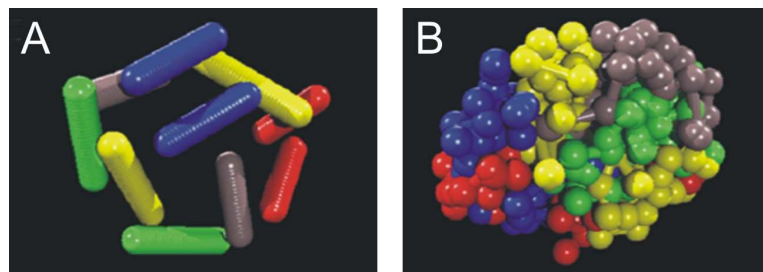


Figure 2. 1 Mb Spherical chromatin domain model. Random distribution of all *Arabidopsis* CTs (A) at the start configuration and (B) after relaxation.

Subsequently, the minimal distances between domains of interest were measured. CTs were considered as associated if boundaries were less than 500 nm apart from each other. At this distance, CTs appear as separated at the microscopic level of resolution. Assuming a distance of 400 nm decreased the expected association frequency of heterologous CTs by no more than 1% and did not alter the significance level for comparison of experimental and simulated data for heterologue association. To test the influence of nuclear shape (flattened sphere, spindle and rod) on random arrangement of CTs, 10^3 nuclei of each shape were modeled. **(Done by G. Kreth and A. Meister)**

2.6.3. Random spatial distribution model

Since the 'SCD' model does not simulate domains <1 Mb, the geometrical 'random spatial distribution' (RSD) model was **established by A. Meister** to simulate spheric chromosome segments of ~100 kb (corresponding to the average BAC insert size) within 10^6 spheric, spindle- or rod-shaped nuclei according to the volumes determined for 2C and 4C nuclei and for the BAC FISH signals ($0.15 \mu\text{m}^3$ and $0.22 \mu\text{m}^3$, respectively) therein. The coordinates of segments were calculated from random numbers. Signals that overlapped or were closer to each other than 100 nm were considered to indicate homologous pairing. The random occurrence of homologous pairing was calculated using the VisualBasic 5.0 (Microsoft) software. The differences between the experimentally obtained values and the simulated ones were compared by the chi-square or Fisher's exact test and considered as significant at the $P < 0.001$ level.

3. Results and discussion

3.1. Establishing of chromosome painting in Arabidopsis thaliana

3.1.1. Development of painting probes for individual chromosomes

Although the Arabidopsis genome consists of only ~15% repetitive DNA arrays (The Arabidopsis Genome Initiative 2000), the presence of BACs containing dispersed DNA repeats has to be avoided carefully when painting probes are arranged since such sequences impair the painting of individual chromosomes by cross-hybridization to other than target chromosomes. In Arabidopsis, repeats are particularly abundant within the (peri)centromeric heterochromatin and the NORs. Therefore, BACs containing (peri-)centromeric or 45S rDNA sequences were omitted from painting probes. Although chromosome arms of most Arabidopsis accessions lack larger blocks of repetitive DNA, visible microscopically as interstitial heterochromatin, complete and truncated mobile elements are scattered along chromosome arms. Painting experiments with chromosome 4 have shown that the use of the complete set of all BACs from the tiling path results in cross-hybridization signals on other chromosomes in addition to painting of chromosome 4 (Lysak et al. 2001). Therefore, a search for repetitive DNA sequences was performed for individual BACs in the TIGR database. BACs containing >5% mobile elements within annotated sequences were omitted from the painting probes, even when sequence in question was found to be restricted to the chromosomal position of the BAC insert. Conversely, some apparently suitable BACs may yield additional FISH signals at other regions. Thus, annotation analysis does not

unambiguously indicate the suitability of BACs for CP. Therefore, individual BACs were additionally spotted on filters and hybridized with radioactively labeled genomic DNA (Figure 3A). BACs yielding strong hybridization signals (Figure 3A) were excluded from painting probes. From the total of 1,585 BACs, 1215 clones (77%) were considered as suitable for CP. Finally the specificity of chromosome specific BAC pools was tested on pachytene chromosomes. At first by two-color CP for the arms of individual chromosomes and then by multi-color CP for entire chromosome complement (Figure 3B,C). For multi-color CP of all five *A. thaliana* chromosomes, in total 73 μ g of labeled DNA per slide were applied (~110 ng of DNA of each of 669 BACs). **[BACs used for painting of chromosomes 1, 2, 3 and 5 were selected by A. Pecinka; clones used for painting of chromosome 4 were selected previously by Lysak et al. (2001)]**

3.1.2. Identification of misaligned BAC clones by FISH

FISH with BACs mapped to the top arm of chromosome 2 yielded signals at other positions than expected. On the basis of signals present elsewhere in the complement, it was found, that at least 14 BACs anchored to the map of the top arm of chromosome 2 were misaligned. For determination of their correct position, individual BACs were hybridized together with a tested correct BAC from the top arm of chromosome 2 to pachytene chromosomes. Two major groups of misaligned BACs were identified: (1) BACs giving a signal on the bottom arm of chromosome 2, and (2) BACs located on another chromosome (Figure 3D). Thus, FISH provides a tool to confirm chromosomal location of individual BACs (see also Schubert et al. 2001).

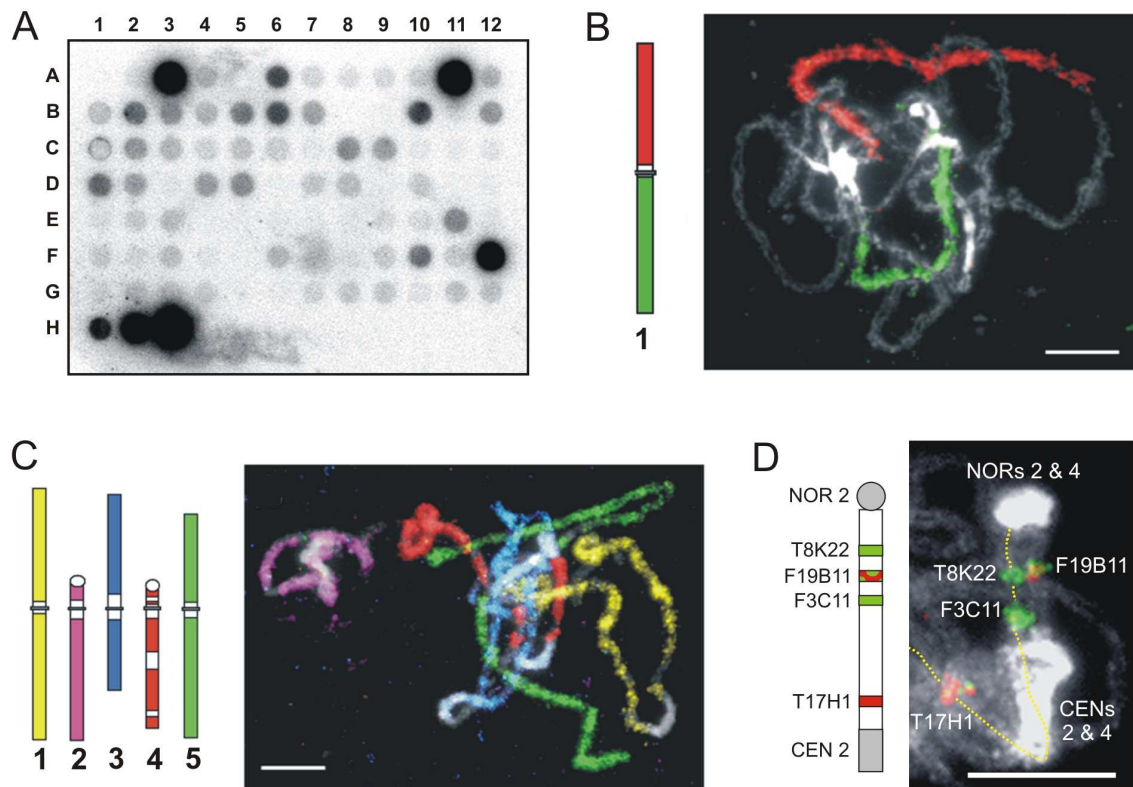


Figure 3. Chromosome painting in *Arabidopsis thaliana*. (A) DNA-DNA dot-blot hybridization of *Arabidopsis* (Col) genomic DNA to 84 BAC clones aligned from A1 to G12 according to their physical position on chromosome 1 (A1 to B4: BACs T22A15 to T28N5; B5 to G12: BACs F25O15 to T7N22); H1 to H3: *Arabidopsis* (Col) genomic DNA (10, 100, 1000 ng); H11,12: water controls. Clones showing a signal intensity stronger than that of C2 were omitted from painting probes. (B) Painting probes were first tested for their specificity to individual chromosomes; exemplified for chromosome 1 schematically (left) and in pachytene (right). The top arm was visualized in red and the bottom arm in green color. (C) Multi-color painting of the five *Arabidopsis* chromosome pairs schematically (left) and in pachytene (right). (D) *In-situ* localization of two misaligned BACs from the top arm of chromosome 2. Left: expected positions of four tested BACs deduced from the physical map of *Arabidopsis* chromosome 2; right: FISH localization of differentially labeled BACs on pachytene chromosomes. The correctly aligned BACs T8K22 and F3C11 (both in green) appear on the top arm of chromosome 2, the misaligned BACs F19B11 (green/red) and T17H1 (red) hybridize to the top arm of chromosome 4 (between the NOR and the heterochromatic knob) and to the bottom arm of chromosome 2, respectively. Chromosomes were counterstained with DAPI. Bars, 5 μ m.

3.1.3. Identification of chromosome rearrangements by means of chromosome painting

The availability of confirmed painting probes allows to detect and visualize induced as well as spontaneous chromosome rearrangements even in species with small and morphologically similar chromosomes such as those of *A. thaliana*. For the transgenic Arabidopsis line T665-IST (Aufsatz et al. 2002), sequencing of the T-DNA insertion site has shown that T-DNA was integrated at the distal end of chromosome 5 bottom arm, upstream of nucleotide 4316 of BAC K9I9. However, the opposite end of the transgene was linked upstream of nucleotide 66153 of BAC F21O3 from the top arm of chromosome 3, suggesting that a reciprocal translocation has occurred during transformation. The position of the chromosome 5 bottom arm terminus (from nucleotide 4317 of BAC K9I9 to the end of the chromosome, in total ~0.2 Mb) was not specified (Aufsatz et al. 2002). To confirm the translocation and to reveal the position of chromosome 5 terminus of the T665-IST genotype, CP was applied. Four differentially labeled contigs arranged according to predicted rearrangement were hybridized to chromosomes of wild-type (Col) and of T-DNA line (Figure 4A). Indeed, contig A (BACs T14P13–T1B9) from the top-arm of chromosome 3 was found to be translocated to the predicted position on chromosome 5. Contig D (K9I9-LA522) from the bottom arm of wild-type chromosome 5 was found at the distal end of the top-arm of chromosome 3, confirming a reciprocal translocation between both chromosomes (Figure 4A).

Furthermore, during experiments with the transgenic Arabidopsis line EL702C (Kato and Lam 2003), a previously not suspected chromosome rearrangement was detected by CP. The line EL702C carries three T-DNAs (~17 kb each) inserted at two loci on the top arm of chromosome 3, ~4.2 Mb apart from each other; the proximal locus harbors two transgenes in inverse orientation (Figure 8A; Kato and Lam 2003). By

FISH with *lac* operator probe (10 kb of transgene) and BACs containing insert sequences internally flanking the transgene loci it was aimed to analyze pairing frequency of the *lac* operator arrays in 2C nuclei (see part 3.3.).

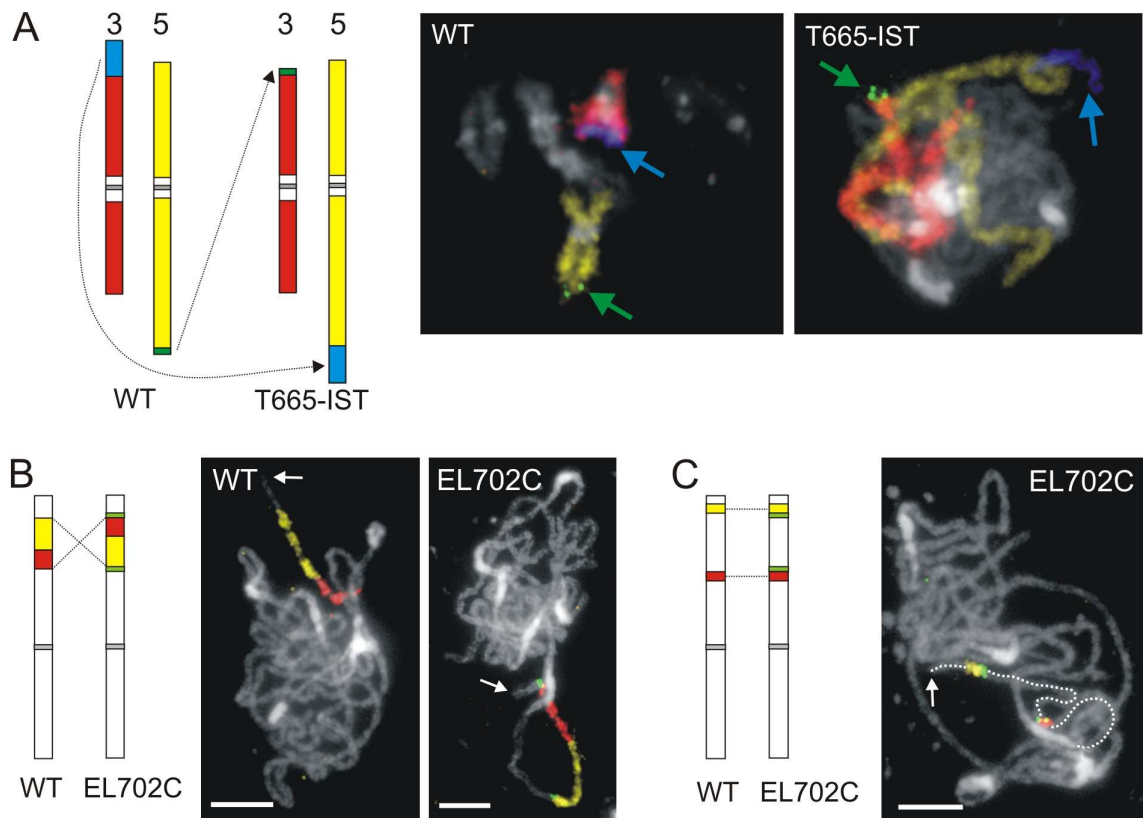


Figure 4. Visualization of chromosome rearrangements by CP. (A) Left: scheme of the reciprocal translocation between chromosomes 3 and 5 in line T665-IST in comparison to wild-type (Col). Right: Chromosome painting of the complex probe to diplotene chromosomes of wild-type and pachytene chromosomes of T665-IST. (B and C) The double transgene insertion in EL702C is accompanied by a paracentric inversion between the integration points. Arrows indicate the top arm end of chromosome 3 bivalent. (B) Painted regions between BACs F2O10 and F28J15 (yellow) and MBK21 and MSL1 (red) schematically positioned on the top arm of chromosome 3 of the wild-type accession Col and, together with the transgene (green), on chromosome 3 of the EL702C genotype. Images show FISH of the complex probe to pachytene chromosomes of wild-type and homozygous EL702C. (C) Regions flanking transgene loci from outwards hybridize in the same order on pachytene chromosomes of wild-type (not shown) and line EL702C. Chromosomes were counterstained with DAPI. Bars, 5 μ m.

To confirm the physical position of the transgene and BAC loci on chromosome 3, differentially labeled probes were first hybridized to pachytene chromosomes of EL702C. The *lac* operator probes hybridized to the predicted locations while the BAC probes hybridized in reversed order suggesting an inversion of the region between the transgene loci. Also FISH with two differently labeled BAC pools (MBK21 to MSL1 corresponding to the upper region and F2O10 to F28J15 corresponding to the bottom region between the insertion loci) yielded signals of reversed orientation on pachytene chromosomes of homozygous EL702C plants compared to the situation in wild-type plants (Figure 4B). FISH signals of BAC inserts flanking the insertion loci externally appeared in the same order on wild-type and EL702C bivalents (Figure 4C), and thus confirmed the inversion between transgenic loci in EL702C plants. However, without sequencing the actual breakpoints (~10 to 55 kb away from the insertions) we are currently not able to identify the molecular event responsible for that inversion and to decide for one of the models proposed for the generation of inversions during insertion of two transgenes in cis (Laufs et al. 1999).

3.1.4. Conclusions as to the chromosome painting in *Arabidopsis thaliana*

Chromosome-specific painting probes were developed for all five chromosome pairs of model plant *A. thaliana* and allowed for the first time differential painting of the entire chromosome complement of a euploid plant. Multi-color FISH with these probes provides a powerful tool for: (i) identification of individual chromosomes, (ii) visualization of chromosome aberrations and (iii) investigation of arrangement and dynamics of *Arabidopsis* chromosomes during interphase and nuclear divisions (Schubert et al. 2001; Lysak et al. 2001, 2003; Pecinka et al. 2004, *J. Cell Sci*,

submitted). Moreover, *A. thaliana* painting probes can be used for comparative studies of interphase chromosome arrangement (A. Berr, A. Pecinka and I. Schubert unpublished data) and of karyotype evolution in closely related *Brassicaceae* species (Lysak et al. 2003, 2005).

3.2. Arrangement of interphase CTs and somatic homologous pairing in nuclei of A. thaliana

3.2.1. The relative positioning of entire CTs is random

Painting probes for differential labeling of all five Arabidopsis chromosomes were hybridized to flow-sorted 4C nuclei from leaves (Figure 5A,B). In agreement with observations in other eukaryotes, chromosome painting revealed three-dimensional, discrete CTs (Figure 5C). To test whether there is a specific side-by-side positioning between individual CTs, association frequencies of all possible homologous and heterologous CT combinations were scored in spheric and spindle-shaped nuclei ($n=51$) and compared with the prediction for their random arrangement according to the SCD model (see Materials and methods, Figure 2, Table 2). The random CT association frequency was calculated as a weighted average of the predicted association values for spheric and spindle-shaped nuclei according to the proportion of evaluated spheric and spindle-shaped nuclei [for original values of the observed and the predicted CT association frequencies (according to the SCD model) for nuclei of different shape see appendix: Tables 7 and 8]. The observed association frequency for all possible combinations ($n=15$) was very high (76.4%-100%), because of the low chromosome number of *A. thaliana* ($2n=10$), and not significantly different ($P>0.05$) from the prediction (68.7%-99.4%) based on 10^3 simulated nuclei.

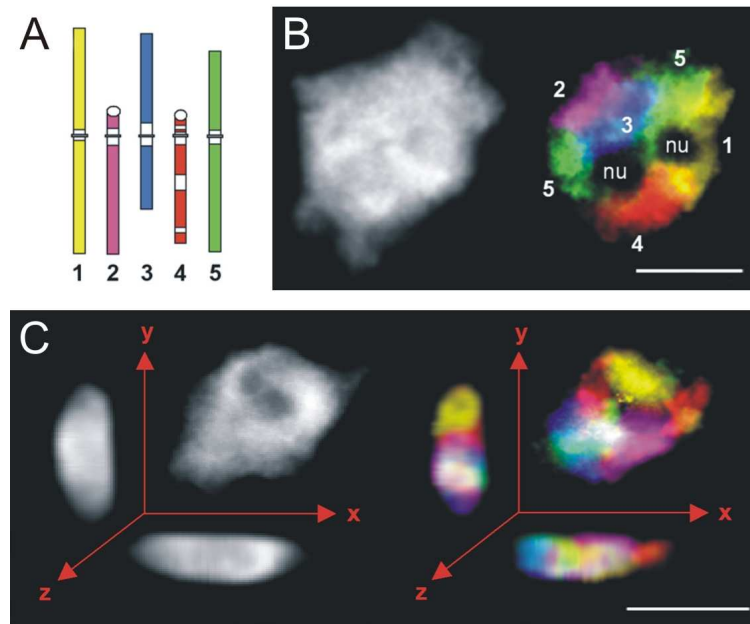


Figure 5. Association of homologous and heterologous chromosome territories. (A) Scheme of differential labeling of individual Arabidopsis chromosomes for multi-color chromosome painting. (B) Central focal plane of a 4C leaf nucleus (left) and of CTs therein painted as in (A) (right); DAPI-stained areas (left) without painting signal correspond to nucleoli (nu) and to the pericentromeric chromocenters containing repetitive DNA sequences that were excluded from painting probes. (C) Maximum intensity projections of a 4C leaf nucleus in three planes, left: DAPI-stained, right: painted chromosome territories as in (A). Bars, 5 μ m.

Table 2 Observed and expected frequency of pair-wise association of all Arabidopsis chromosome territories in 4C leaf nuclei

Chromosome combination	Association frequency (%) ^{a)}	
	<i>A. thaliana</i> Col ($n=51$)	SCD model ($n=10^3$)
1-1	88.2	85.3
1-2	96.1	99.1
1-3	100.0	99.4
1-4	98.0	98.8
1-5	100.0	99.4
2-2	76.5	74.8
2-3	96.1	98.6
2-4	96.1	98.3
2-5	98.0	98.8
3-3	80.4	77.5
3-4	96.1	98.4
3-5	98.0	98.5
4-4	78.4	68.8
4-5	96.1	97.5
5-5	88.2	78.8

^{a)} all differences between observed and simulated values were not significant ($P>0.05$) in Fisher's exact test.

No obvious preference as to the radial arrangement of specific CTs was observed. A large proportion of all CTs (preferentially the heterochromatic chromocenters) touched the nuclear envelope. The lack of a specific radial arrangement of entire CTs is most likely due to the low number and similar size of Arabidopsis chromosomes (The Arabidopsis Genome Initiative 2000). However, to a certain extent radial positioning might be present at subchromosomal level, since the heterochromatic pericentromeric chromocenters are often located at the nuclear periphery, while telomeres cluster around the nucleolus (Fransz et al. 2002).

3.2.2. The association frequency of homologous chromosome arm territories is random for chromosomes 1, 3, 5 and higher for chromosomes 2 and 4

To test whether the random relative positioning, found for the entire chromosomes, holds true also for homologous chromosome arms, painting experiments with probes specific for the arms of all individual chromosomes were performed.

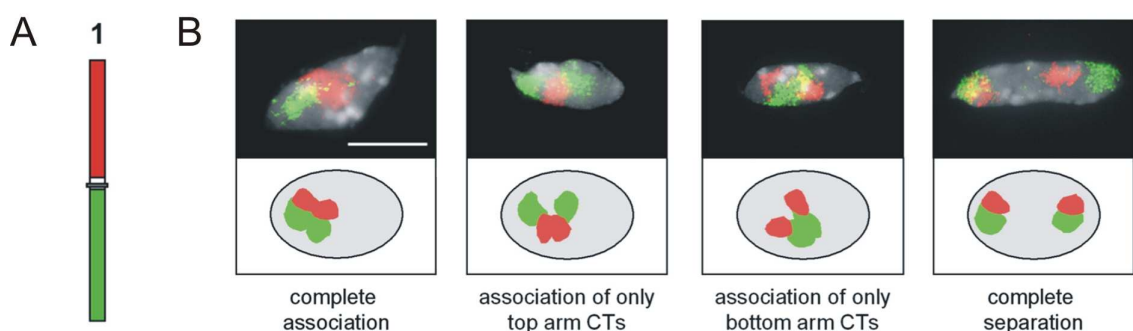


Figure 6. Association of homologous chromosome arm territories. (A) Scheme showing differential labeling of chromosome 1 top (*red*) and bottom (*green*) arm. (B) The four types of arrangement of homologous chromosome arm territories (exemplified for chromosome 1) as images of central focal planes of 4C leaf nuclei (upper part) and schematically below. Bar 5 μm .

Either spatial association of both arms, of only the top arms, of only the bottom arms or complete separation of homologous territories was distinguished and recorded (Figure 6). Simulations of random arrangement of homologous CTs were performed according to the SCD model (Figure 2). Because in Arabidopsis roots and leaves three nuclear shapes (flattened sphere, spindle, rod; Figure 1) occur frequently, independent simulations were done (10^3 nuclei per shape) to test whether an influence of the nuclear shape on CT arrangement is to be expected. Indeed, the simulations revealed an impact of nuclear shape on the random association frequency of CTs. For the symmetric chromosomes 1, 3, and 5 the computer model predicted association of entire homologues in 48.3-59.9% of spheric nuclei, in contrast to only 20.6-23.6% of rod-shaped nuclei. For the asymmetric chromosomes 2 and 4 the predicted values were 25.2-31.9% and 14.8-18.7%, respectively. Because of the predicted differences, we merged the values simulated for different nuclear shapes by calculation of the weighted average according to the proportion of evaluated spheric, spindle and rod-shaped nuclei per experimental point [for original values of the observed and the predicted CT association frequencies (according to the SCD model) for nuclei of different shape see appendix: Tables 9 and 10]. These values were compared with the sum of values for all shapes per experimental point (Table 3). The observed association frequency (Figure 6, Table 3) did not significantly deviate from the SCD model prediction for random arrangement in the case of chromosome 1. This was valid for the differently shaped nuclei of 2C, 4C, and 8C DNA content from roots as well as from leaves. Corresponding data were obtained for chromosomes 3 and 5 as studied in 4C leaf nuclei (Table 3). Different observations were made for the smaller asymmetric chromosomes 2 and 4 with NORs at their top arm ends. For both these chromosomes the association of entire homologues occurred significantly more often ($P < 0.001$) and complete separation less often than expected at random in all tested types of nuclei. This increase of

association also holds true when considering the values for entire homologues and for only top arms (T+B+ and T+B-) together and becomes even more pronounced with an increasing ploidy (Table 3). The significant increase in association frequency of homologous entire and top arm territories of chromosomes 2 and 4 is apparently due to the frequent attachment of the NORs to a single nucleolus (in >90% of nuclei) in a way mediating association of homologues.

Table 3 Association frequencies of homologous chromosome-arm territories in leaf and root nuclei of different ploidy levels^{a)}; T=top arm, B=bottom arm, +=associated, -=separated

Homologues	<i>A. thaliana</i> Columbia							SCD model ($n=10^3$)				χ^2 test ^{b)}
	n	Organ	Ploidy	Association frequency (%)				Association frequency (%)				
				T+B+	T+B-	T-B+	T-B-	T+B+	T+B-	T-B+	T-B-	
Chromosome 1	121	leaf	2C	47.1	19.8	14.9	18.2	55.0	12.3	13.8	18.9	-
	100		4C	47.0	20.0	12.0	21.0	48.5	11.3	12.5	27.7	-
	101		8C	42.6	16.8	13.8	26.8	50.6	11.5	12.6	25.4	-
	120	root	2C	37.5	15.8	13.4	33.3	39.0	10.4	11.4	39.2	-
	120		4C	35.0	29.2	24.2	11.6	33.3	26.7	33.3	6.7	-
	120		8C	45.8	15.0	14.2	25.0	47.6	10.9	11.9	29.6	-
Chromosome 2	120	leaf	2C	45.8	6.7	19.2	28.3	31.1	2.5	36.2	30.2	***
	120		4C	45.0	5.8	22.5	26.7	30.6	2.4	36.0	31.0	***
Chromosome 3	102	leaf	4C	47.0	26.5	6.9	19.6	43.6	20.3	6.7	29.4	-
Chromosome 4	120	leaf	2C	42.5	3.3	25.8	28.4	21.3	1.2	35.6	41.9	***
	120		4C	39.2	10.0	26.7	24.1	23.1	1.4	40.8	34.7	***
	111		8C	42.0	21.4	10.7	25.9	21.3	1.2	35.3	42.2	***
	120	root	2C	39.2	8.3	23.3	29.2	19.2	1.0	29.3	50.6	***
	122		4C	43.4	6.6	19.7	30.3	19.7	1.1	31.0	48.3	***
	130		8C	45.4	25.3	10.8	18.5	21.0	1.1	34.2	43.6	***
Chromosome 5	115	leaf	4C	49.6	11.3	20.0	19.1	46.5	8.9	17.4	27.2	-

^{a)} Per experimental point the percentage of observed values for the sum of spheric, spindle and rod-shaped nuclei is given and compared to the SCD model prediction based on the weighted average for the three nuclear shapes.
^{b)} Significance level of differences between the entirety of observed versus expected values per experimental point in a column-wise comparison: - $P>0.05$; *** $P<0.001$;
For individual columns (observed versus model): bold $P<0.001$, bold italics $0.001<P<0.05$.

The pronounced increase of total top arm association (T+B+ and T+B-) in 4C and 8C leaf and root nuclei is paralleled by a decrease in the average number of FISH signals for 45S rDNA per nucleus from 3.0 in 2C to 1.6 in 8C nuclei (Z. Jasencakova and I. Schubert unpublished data). However, the enhanced fusion of NORs in polyploid nuclei, does not affect homologous association frequency of the bottom arms (T-B+). A ‘strong tendency’ for association of homologues (in 53%-70% of nuclei) was found in

human Sertoli cells (Chandley et al. 1996). However, among the tested chromosomes only the acrocentric NOR-bearing chromosomes 13 and 21 showed a high frequency of homologous association (50%) also in dividing lymphocytes, apparently due to attachment of NORs at one nucleolus (Chandley et al. 1996).

In 8C nuclei, in general no more than two CTs were found per homologue. Also the number of chromocenters (at maximum 14, i.e. 10 pericentromeres and 4 NORs, but usually not more than 10, Fransz et al. 2002) did not significantly increase in >4C nuclei. Both observations suggest that CTs of endoreduplicated chromatids are usually not separated but remain associated, at least within the pericentromeric regions.

3.2.3. The relative position of a gene (*FWA*) within its CT does not necessarily reflect the transcriptional state

After FISH with differently labeled probes for the chromosome 1 top arm territory and for BAC T2P11 therein (probe contained BACs flanking BAC T2P11 directly from the both sides) to 4C leaf nuclei ($n=359$), 12.8% of FISH signals for the BAC were localized clearly outside the labeled CT. This surprising observation provoked the question, whether the FISH signal for the corresponding BAC apart from the remaining CT is due to an outlooping correlated with the transcriptional activity of genes in the labelled region.

To test whether the transcriptional activity might have an impact on CT organization, i.e. whether a transcribed gene occupies more often positions outside compact CT than under silent condition, the flowering gene *FWA* residing in BAC M7J2 and mapped to the bottom arm of chromosome 4 was chosen. In wild-type plants (*Ler*) this gene is not expressed and strongly methylated, while it is constitutively expressed and hypomethylated in leaf nuclei of the *fwa-1* mutant (Soppe et al. 2000). In

2C leaf nuclei ($n=337$) of *fwa-1* only 4.2% of FISH signals for BAC M7J2 were found distal of the CT periphery (Figure 7A). A similar frequency (3.8%) of signals out-looped from the CT was observed also for wild-type 2C leaf nuclei ($n=368$). In 4C nuclei, out-looping of M7J2 signals occurred in 10.7% of *fwa-1* nuclei ($n=121$) and in 6.5% of 230 wild-type nuclei ($n=230$). Although there is a tendency of more out-looping in *FWA*-expressing 4C nuclei, the difference is not significant.

Thus, the position of a sequence relative to its CT (inside, at the edge or outside) does not obviously depend on the transcriptional state of that sequence. This agrees with the observations made on mammalian cells where active genes were found to be located on the surface as well as in the interior of a CT and were not relocated when switching the expression status (Mahy et al. 2002a). Therefore, transcriptional activity of a gene is not necessarily a reasonable explanation for the relatively high frequency (12.8%) at which the FISH signal for BAC T2P11 was found ‘outside’ the chromosome 1 top arm territory. However, regions of ‘high gene density and transcription’ may frequently extend from their territory (Mahy et al. 2002b) as already described for the major histocompatibility complex region that may locate outside its CT depending on cell type and gene activity (Volpi et al. 2000). The gene density along Arabidopsis chromosome arms is rather uniform, but we cannot exclude that most of the 21 presumed genes of BAC T2P11 are simultaneously expressed in nuclei showing this region apart from its CT. The results obtained with BACs T2P11 and M7J2 imply that CTs do not always have a smooth surface, i.e. outlooping of chromatin into interchromosomal space (mimicking intermingling of CTs) might occur to some extent. **(Preparation of chromosome painting probes and approximately one half of FISH experiments were done by A. Pecinka; the remaining part and microscopic evaluations were done by V. Schubert).**

3.2.4. Somatic pairing of homologous chromosome segments occurs at random

To analyze whether association of homologous CTs reflects strict allelic alignment along chromosome pairs, the nuclear positions of ~100 kb chromosome segments (average BAC insert size) were assessed by FISH. Simultaneous detection with differentially labeled probes of the chromosome 1 top arm territory and of BAC T2P11 therein has shown that of 94 4C leaf nuclei with associated top arm territories only 7 also showed homologous pairing at the position of the T2P11 insert (one FISH signal for T2P11, Figure 7B₁). This indicates that association of homologues is not a consequence of homologous alignment. **(CP probes were prepared by A. Pecinka; FISH and microscopic evaluation were done by V. Schubert).**

Pairing was further analysed for different regions on chromosomes 1, 3 and 4 using either single BACs or two differently labeled adjacent BACs for FISH (Figure 7C). A single compact signal site per nucleus was regarded as single-point pairing in contrast to clearly separated signals indicating the absence of pairing (Figure 7D_{1,2}). In addition, in some experiments (Table 4) nuclei that contained dispersed signals of spheric shape or separated compact signals with a distance less than the signal diameter (Figure 7D₃) were scored. Such nuclei were considered to represent a loose signal association indicating spatial vicinity but not necessarily allelic alignment of homologous segments. The RSD model simulations of 10⁶ 2C and 4C root and leaf nuclei, respectively, predicted a random frequency of 5.9-7.8% of nuclei with homologous pairing (Table 4). In contrast to the situation described for association of CTs, computer simulations revealed no significant differences as to the random expectation of single-point pairing for the three predominant nuclear shapes (sphere, spindle, rod). The reason is presumably that FISH signals for ~100 kb segments occupy a much smaller proportion of the nuclear volume and therefore cause less spatial

constraints than do CTs. The observed frequency of nuclei showing single-point pairing at the tested positions (0.8-14.0%; on average 4.9%; Table 4) was 7-10 times lower than that for association of both arms of the corresponding homologous pair (35.0-49.6%; Table 4).

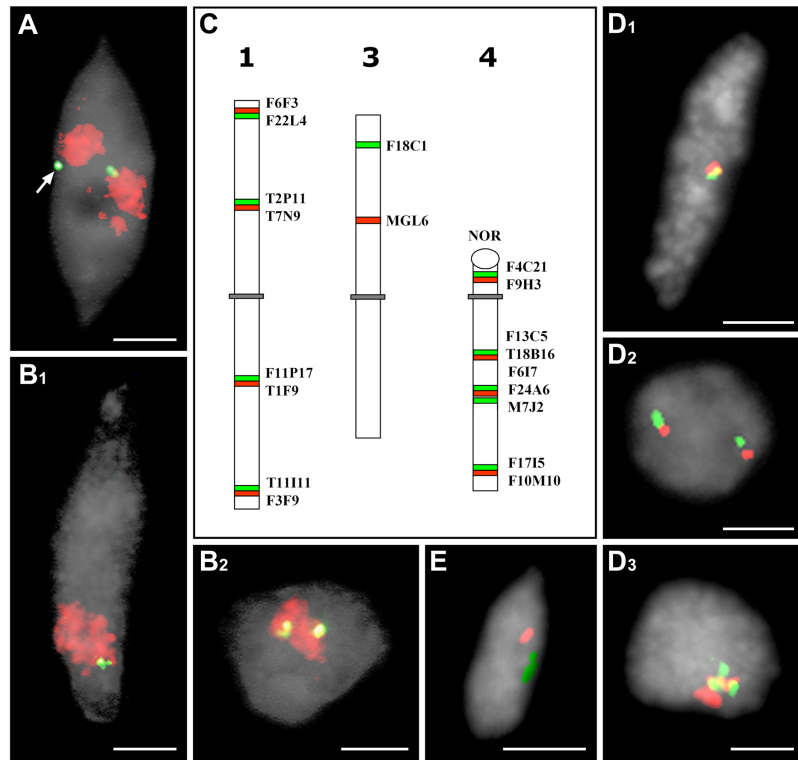


Figure 7. Relative position (to each other/their CTs) of homologous ~100 kb chromosome segments. (A) 2C leaf nucleus of the *fwa* mutant with separated chromosome 4 bottom arm territories painted in red and an ~80 kb chromosome segment of the same arm (BAC M7J2 in green); one segment (arrow) looped out from its territory. (B) 4C wild-type (Col) leaf nuclei with associated chromosome 1 top arm territories painted in red and therein a ~85 kb chromosome segment (BAC T2P11 in green) paired (B₁) or separated (B₂). (C) Scheme of chromosomes 1, 3 and 4 indicating the BAC sequence positions used for analysis of single-point pairing by FISH. (D) Single-point pairing of the segments T2P11/T7N9 in a 4C root nucleus (D₁), separation of the homologous segments F11P17/T1F9 in a 2C leaf nucleus (D₂) and loose spatial association of the segments T2P11/T7N9 in a 4C root nucleus (D₃) based on compact (D₁ and D₂) and dispersed signals (D₃). (E) Rare simultaneous pairing of two homologous segments (F9H3;F17I5) from opposite arms of chromosome 4 in a 2C root nucleus. Nuclei were counterstained with DAPI. Bars, 3 μm.

Table 4 Single-point homologous chromosome pairing and segment association analysed by FISH with BAC pairs or single BACs in nuclei of different organs and ploidy levels in comparison to the RSD model

	BACs	Organ	Ploidy	n_1	Pairing frequency (%) ^{a)}	n_2	Pairing + association frequency (%)	
Chromosome 1	F6F3/F22L4	Leaf	2C	299	4.3	379	24.5	
			4C	355	5.4	443	24.2	
		Root	2C	357	4.2	435	21.4	
			4C	265	8.3	343	29.1	
	T2P11/T7N9	Leaf	2C	299	8.0	362	24.0	
			4C	571	2.1 ***	670	16.6	
		Root	2C	243	5.3	264	12.9	
			4C	603	0.8 ***	659	9.3	
	F11P17/T1F9	Leaf	2C	141	4.3	171	21.2	
			4C	328	1.8 ***	382	15.6	
		Root	2C	436	3.7 ***	503	16.5	
			4C	476	4.8	530	14.5	
	T11I11/F3F9	Leaf	2C	487	4.3	615	24.2	
			4C	374	4.5	505	31.5	
		Root	2C	528	7.0	631	22.2	
			4C	544	3.9	646	19.0	
	Chromosome 3	F18C1	Leaf	2C	134	5.2	153	17.0
		MGL6	Leaf	2C	141	4.3	153	11.7
Chromosome 4	F4C21/F9H3	Leaf	2C	104	9.6			
			4C	114	3.5			
		Root	2C	109	10.3			
			4C	120	6.7			
	F9H3	Leaf	2C	189	7.4	222	21.2	
		Root	2C	265	5.7	308	18.8	
	F13C5/T18B16	Leaf	2C	107	3.7			
			4C	121	5.0			
		Root	2C	113	14.0			
			4C	116	1.7			
	F6I7/F24A6	Leaf	2C	113	6.2			
			4C	119	3.4			
		Root	2C	92	13.3			
			4C	113	5.3			
	M7J2 ^{b)}	Leaf	2C	315	4.8	368	18.6	
			4C	207	1.9	230	11.7	
	F17I5/F10M10	Leaf	2C	118	7.6			
			4C	120	1.7			
		Root	2C	109	11.1			
			4C	115	5.2			
F17I5	Leaf	2C	199	5.5	222	15.4		
	Root	2C	255	9.0	308	24.7		
RSD model ^{c)}	Leaf	2C	10 ⁶	7.8				
		4C	10 ⁶	6.9				
	Root	2C	10 ⁶	7.4				
		4C	10 ⁶	5.9				

^{a)}Compare with the simulated random values according to the RSD model below; *** $P < 0.001$.

^{b)}Only this BAC was tested in *Ler* and not in *Col* background.

^{c)}On the basis of differences in volumes of 2C and 4C root and leaf nuclei (see Appendix: Table 6), four expected pairing frequencies were calculated for comparison with the experimental data.

n_1/n_2 : For 9 positions along chromosomes 1, 3 and 4 in addition to nuclei showing either strict punctual pairing or clear separation ($\Sigma=n_1$), nuclei with stretched signals of dispersed appearance or with compact signals of a distance less than the signal diameter (together considered as 'association') were scored separately and added to n_1 ($\Sigma=n_2$).

Compared to pairing, a signal association is up to 10 times more frequent. Adding the number of nuclei showing single-point pairing to that showing loose association revealed that, depending on the chromosomal position, within 9.3 to 31.5% of nuclei allelic sequences occur in a close spatial proximity (Table 4). Regardless of the chromosomal position, pairing was not observed significantly more often than expected at random according to the RSD model. No significant differences were found between leaf and root nuclei irrespective of the ploidy level (tested for chromosomes 1 and 4). Thus, in *A. thaliana* nuclei somatic pairing is the exception rather than the rule. The opposite has been shown for *Drosophila melanogaster* with homologous pairing in 60%-90% of somatic nuclei from the 13th embryonic cell cycle on (Csink and Henikoff 1998; Fung et al. 1998). The comparison of Arabidopsis and Drosophila shows that similarity in genome size, sequence organization and chromosome number does not necessarily cause an identical CT arrangement. of the constraints as to the chromatin dynamics within interphase nuclei of all tested organisms, a certain flexibility of chromatin positions has been found (for review see Lam et al. 2004). The average movement of GFP-tagged chromatin loci is $\sim 0.085\mu\text{m}/\text{min}$ (Kato and Lam 2003). Therefore, at least in nuclei that show either single-point pairing or close association of allelic sequences, these allelic sequences might occupy nuclear positions sufficiently close for homologous recombination (for instance in the course of double strand break repair), in spite of the lack of a regular and contiguous alignment of homologues.

For chromosome 1 the positional proximity of allelic sequences (single-point pairing and segment association together) was less pronounced at interstitial loci (15.0% on top arm; 16.1% on bottom arm) than at distal loci (24.6% on top arm; 23.8% on bottom arm) when all data from 2C and 4C, leaf and root nuclei were pooled ($P < 0.001$). This agrees with the clustering of telomeric regions around the nucleolus (Fransz et al. 2002).

Simultaneous FISH of two BACs located distantly on a chromosome showed that homologous pairing has indeed only single point character and does not involve entire chromosomes (tested for four independent combinations: F6F3 and T11I11; T7N9 and F11P17; F18C1 and MGL6; F9H3 and F17I5; Figure 7C). Only three (0.2%) out of 1240 tested nuclei showed simultaneous pairing at two distant loci (Figure 7E). **(Experiments with BACs from chromosome 1 and approximately one-third of experiment with BACs from chromosome 4 were done by V. Schubert; experiments assessing pairing of BACs from chromosome 4 were performed by M. Klatte; experiments with BACs from chromosome 3 were done by A. Pecinka.)**

3.2.5. The frequency of somatic homologous pairing is not altered in Arabidopsis mutants with an increased frequency of somatic homologous recombination

Intermolecular recombination plays an important role in DNA repair of somatic cells and is essential for the elimination of damaged DNA. To study the frequency of intermolecular recombination events between homologous chromosomes and sister chromatids, transgenic Arabidopsis lines carrying a specially designed recombination trap consisting of disrupted a β -glucuronidase reporter gene in a direct repeat orientation were generated (Molinier et al. 2004). In case of a recombination event between the direct repeats of a marker gene, a functional reporter gene is restored. Three mutant lines B71, W92 and P8I24 displayed a significantly (>40-fold) increased frequency of somatic homologous recombination in comparison to the control line IC9 (J. Molinier and B. Hohn, unpublished data). Similar results were obtained for the *Atp150caf-1* mutant with a T-DNA insertion in the middle of the *AtCAF-1* encoding region. This mutant showed a >100-fold increased frequency of somatic homologous recombination

compared to the control line C24 (Kyryk, Pecinka, Wendeler, Kemper and Reiss, manuscript in prep.).

These results together led to the question, whether the higher frequency of somatic homologous recombination found in B71, W92, P8I24 and *Atp150caf-1* might be due to a generally increased pairing frequency between homologues, or rather to an intensified search for homology to repair induced or spontaneous DNA damage. To elucidate this issue, the single-point pairing frequency was addressed by FISH in 2C leaf nuclei of hyperrecombination mutants and their control lines. The attempt to assess pairing frequency directly at the transgenic locus was not possible because of: (i) the relatively small size of T-DNA construct (only 5.6 kb), which did not allow a reliable microscopic detection of FISH signals and (ii) the unknown position of the transgene in the genome which excluded the use of a neighboring BAC insert as a probe. Therefore, the analyses were performed with two BACs, F18C1 and MGL6 (see parts 3.2.4. and 3.3.3.), from the top arm of chromosome 3 (Figure 7C).

Table 5 Single-point homologous chromosome pairing analysed by FISH with single BACs in nuclei of different hyperrecombination mutants and of corresponding control lines.

Genotype	Organ	Ploidy	Analyzed nuclei	Homologous pairing frequency (%)	
				BAC MGL6	BAC F18C1
IC9	Leaf	2C	150	6.0	5.3
P24I8	Leaf	2C	150	6.0	4.0
B71	Leaf	2C	150	6.0	4.7
W92	Leaf	2C	150	5.3	5.3
C24	Leaf	2C	150	4.0	4.6
<i>Atp150caf-1</i>	Leaf	2C	186	4.8	5.3

The frequency of nuclei showing single-point pairing (on average 5.3%; Table 5) did not deviate between mutants and their control lines was similar to that for average euchromatic regions in wild-type nuclei of *Arabidopsis* (Col) (see Table 4). Therefore, the increased frequency of somatic homologous recombination found in mutants B71,

W92, P8I24 and *Atp150caf-1* is not associated with an elevated frequency of somatic homologous pairing.

The data from b-glucuronidase assay suggest that homologous chromosomes as well as sister chromatids, can be used as a substrate for somatic homologous recombination in *Arabidopsis* nuclei (Molinier et al. 2004). Interestingly, sister chromatids are used 2-3 times more often for somatic recombinational repair than homologous chromosomes (Molinier et al. 2004). The frequent use of homologues in somatic recombination is in contrast to the low frequency of somatic homologous pairing in *Arabidopsis* nuclei and suggests a mechanism leading to an intensified search for homology after induced or spontaneous DNA damage. Such a search could be catalyzed in *Arabidopsis* by some protein(s) from the RAD52 epistasis group [i.e. RAD51, RAD52, RAD54, RAD55, RAD57 and the MRN (MRE11-RAD50-NBS1 complex)] (West et al. 2004).

3.2.6. Conclusions as to the arrangement of interphase CTs and somatic homologous pairing

Using chromosome specific painting probes, arrangement and dynamics of all *Arabidopsis* interphase CTs was studied in 2C, 4C and 8C nuclei isolated from roots and leaves. Individual CTs were found to be frequently associated with any other CTs. However, this arrangement corresponds to the computer model prediction for random CT arrangement and is most likely due to the low number of *Arabidopsis* chromosomes ($2n=10$). The only exceptions are the NOR-bearing top arms of chromosomes 2 and 4, which associate more frequently than expected at random. This is probably caused by frequent attachment of NORs to a single nucleolus (in >90% of *Arabidopsis* nuclei), which mediates association of homologous NOR-bearing chromosome arms and of

entire homologues. In general, this arrangement was consistent in all investigated types of nuclei. Furthermore, the relative position of a gene (*FWA*) within its CT (inside or at the periphery) does not obviously correlate with its transcriptional state. Somatic homologous pairing occurred on an average in 4.9% of Arabidopsis nuclei. This is in agreement with the computer model prediction for random positional pairing frequency (5.9-7.8%). Only in 0.2% of nuclei, simultaneous homologous pairing of two segments at distant chromosomal positions was found. Thus, homologous pairing has only single-point character and long range homologous alignment seems to be the exception rather than the rule in Arabidopsis nuclei. No significant differences as to the frequency of homologous pairing were found in Arabidopsis mutants with an increased frequency of somatic homologous recombination. This suggests that the observed increase in recombination frequency is rather due to more intensified search for homology after DNA damage than to gross alterations of nuclear organization.

The comparison of Arabidopsis and Drosophila (the latter species is characterized by frequent somatic homologous pairing) shows that similarity in genome size, sequence organization and chromosome number does not necessarily cause an identical arrangement of interphase chromosomes. Therefore, the arrangement of Arabidopsis CTs seems to be more similar to that found in nuclei of non-cycling mammalian cells that are characterized by predominantly random relative positioning of CTs (Cornforth et al. 2002). However, in contrast to nuclei of vertebrates, no pronounced radial arrangement of CTs could be found in Arabidopsis. This is apparently due to the small number of Arabidopsis chromosomes and their similar gene density.

3.3. Alteration of the local interphase chromosome arrangement by tandem repetitive transgenes and fluorescent chromatin tags

3.3.1. GFP spot numbers vary in 2C live nuclei of homozygous transgenic plants (EL702C) harboring two tagged loci on the top arm of chromosome 3

The transgenic *Arabidopsis* line EL702C carries three *lac* operator/GFP-lacI-NLS transgenes (~17 kb each) inserted at two independent loci on the top arm of chromosome 3, ~4.2 Mb apart from each other (Figure 8A). The proximal locus harbors two transgenes in inverse orientation.

In live 2C guard cell nuclei of homozygous EL702C plants, Kato and Lam (2003) only rarely observed four GFP spots. For statistical evaluation, they counted GFP spot numbers in live guard cell nuclei of cotyledons of hemizygous and homozygous EL702C plants and of homozygous EL700S plants (Figure 8B,C). Since EL700S plants contain the same construct as EL702C plants except for the *lac* operator array, homogeneously distributed GFP signals but no GFP spots were expected in the nucleoplasm. In hemizygous EL702C plants Kato and Lam (published in Pecinka et al. 2005) found 5% of 92 nuclei without spots, 66% with one spot, 27% with two and 2% with three spots. In homozygous EL702C plants 12% of 197 nuclei were without spot, 34% showed one spot, 37% two, 11% three and 6% four spots. In homozygous EL700S plants, 55 out of 56 nuclei showed no, and one nucleus (<2%) showed one spot. The single spot observed in an EL700S nucleus and a third spot in two hemizygous EL702C nuclei were most likely caused by spontaneous aggregation of GFP-lac repressor-NLS molecules. The absence of GFP spots in some EL702C nuclei might be due to a high level of unbound GFP-lac repressor-NLS protein yielding a strong overall fluorescence intensity that

prevents discrimination of spots at the tagged loci. **(this initial experiment was performed by N. Kato)** The less than expected numbers of GFP spots in several nuclei of homozygous and hemizygous EL702C plants indicated either frequent association and/or a lack of appearance of GFP spots in these nuclei. To distinguish between these options, FISH experiments were performed to trace individual *lac* operator loci with and without expression of the GFP-lac repressor.

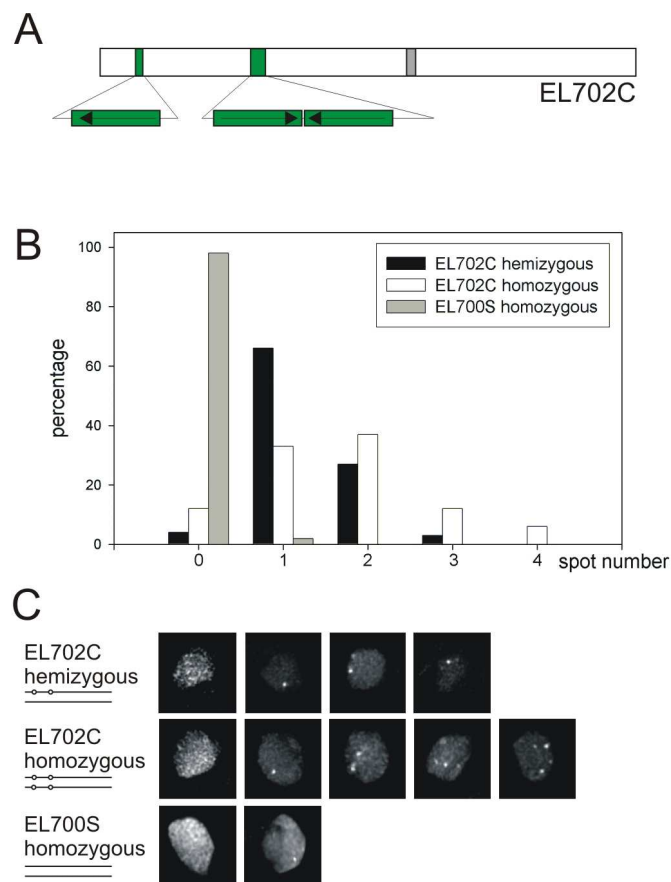


Figure 8: GFP spot numbers in living guard cell nuclei (2C) from cotyledons of dexamethasone-treated transgenic seedlings. (A) Scheme of chromosome 3 with position of transgene insertions (indicated in green) in EL702C line. The proximal locus harbors two transgenes in inverse orientation. (B) Percentage of nuclei with 0, 1, 2, 3, and 4 spots of hemizygous EL702C plants ($n=92$), of homozygous EL702C plants ($n=197$) and of homozygous EL700S plants ($n=56$). (C) Representative images of nuclei with 0, 1, 2, 3, or 4 spots from each of the lines and schematic view of the *lac* operator array loci on chromosome 3 in each line.

3.3.2. GFP spots always co-localize with FISH signals of *lac* operator arrays, but not vice versa

At first, GFP spots and FISH signals of the *lac* operator repeats were counted in flow-sorted 2C nuclei of homozygous EL702C plants, in which expression of the GFP-*lac* repressor protein was induced with dexamethasone (Dex) (Figure 9). Nuclei without clear GFP spots were excluded from evaluation. Out of 63 analyzed nuclei, 30% showed one, 35% two, 25% three and 10% four GFP spots. In contrast, 22% of nuclei showed four FISH signals, 35% two, 35% three and 8% showed one FISH signal (Figure 9A). All GFP spots coincided with a *lac* operator FISH signal (Figure 9B), but not *vice versa*.

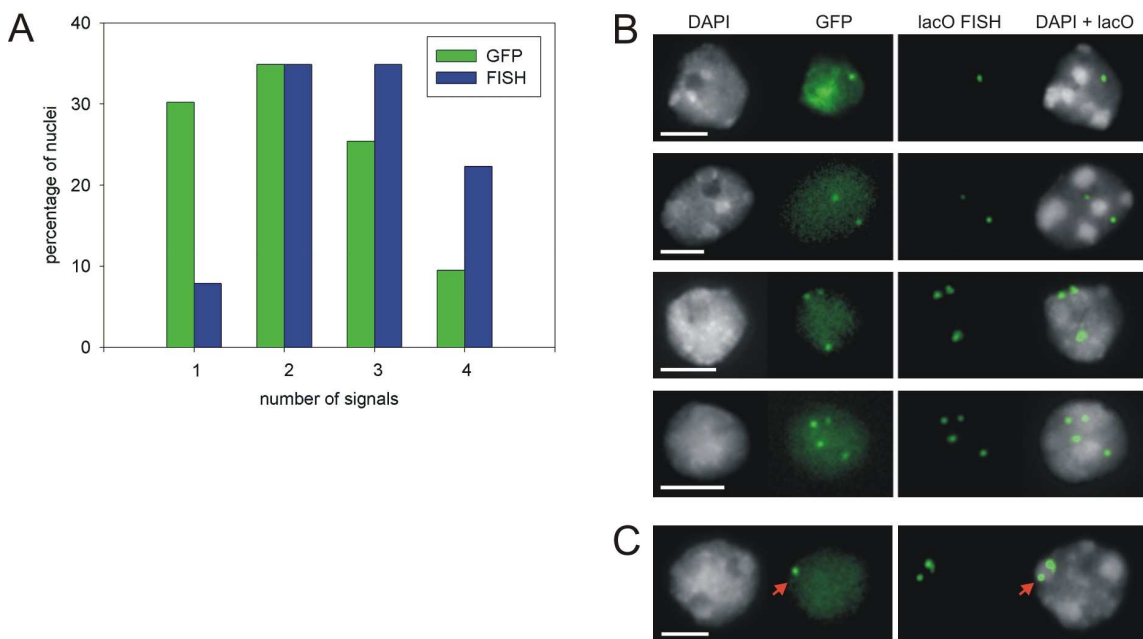


Figure 9. Co-localization of GFP-spots and *lac* operator-FISH signals in Dex-treated 2C leaf nuclei of homozygous EL702L plants. (A) Percentage of nuclei with 1 to 4 GFP spots versus FISH signals. There may occur less GFP spots than FISH signals in one nucleus. (B) Examples of nuclei with 1, 2, 3 or 4 GFP spots coinciding with *lac* operator-FISH signals. (C) Example of a nucleus with missing GFP spot (arrow). Nuclei were counterstained with DAPI. Bars, 3 μ m.

In total 83% out of 252 FISH signals coincided with a GFP signal. Thus, 17% of the transgene loci cannot be detected by a GFP spot in Dex-treated homozygous EL702C nuclei under the applied conditions (Figure 9C). Apparently, some GFP spots could not be discriminated because of high overall fluorescence intensity and/or rapid bleaching of signals within a minute of exposure. Less than 4 FISH signals per nucleus may be most likely due to ectopic or allelic alignment of the *lac* operator arrays.

3.3.3. *Lac* operator arrays pair more often than random in nuclei of transgenic plants and thus enhance pairing frequency of adjacent endogenous regions

To test whether the lower than expected number of signals for *lac* operator arrays is indeed due to homologous pairing, FISH experiments with the *lac* operator array and BACs flanking the transgenic loci were conducted. The pairing frequency of the *lac* operator arrays was assessed by tri-color FISH with BAC MGL6 (79.5 kb, ~54 kb downstream of the insertion, red) flanking the distal locus, BAC F18C1 (100.8 kb, ~55 kb upstream of the insertion, yellow) flanking the proximal locus and *lac* operator probe (green) (Figure 10B-D), in 60 hemizygous untreated, 62 homozygous untreated and 59 homozygous Dex-treated EL702C nuclei. The *lac* operator array alignments were classified as two different types of homologous pairing. If two signals (MGL6, red and F18C1, yellow) co-localized with a *lac* operator signal (green), the alignment was identified as ectopic pairing. If all signals of either MGL6 or F18C were co-localized with a *lac* operator signal, the alignment was identified as allelic pairing. In hemizygous nuclei, ectopic pairing was detected for 13% of the *lac* operator loci without Dex-treatment. In homozygous EL702C nuclei without Dex-treatment, ectopic pairing was observed for 27% of the *lac* operator array loci and allelic pairing for 34% of the loci. After Dex-

treatment, these values increased to 35% (ectopic pairing, $P=0.052$) and 45% (allelic pairing, $P=0.017$), respectively (Figure 10A).

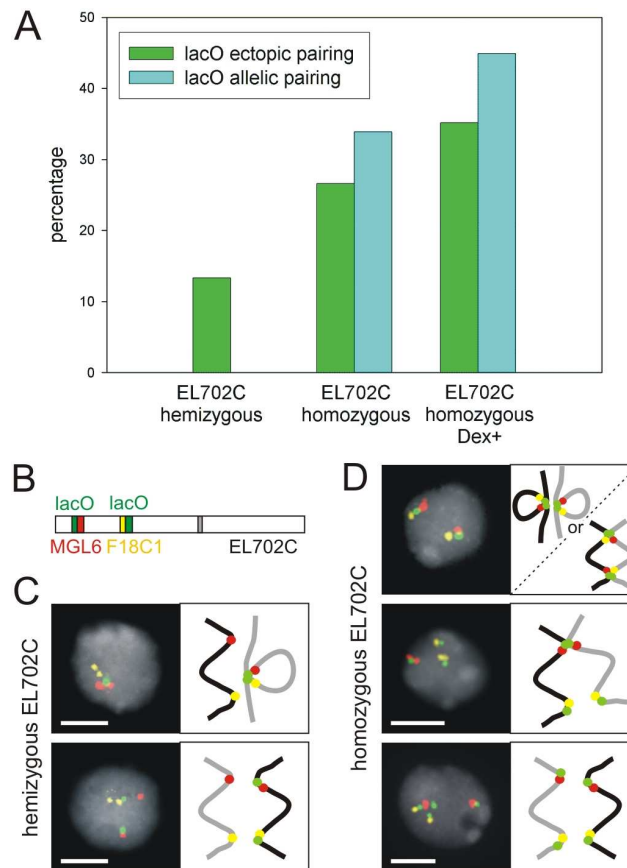


Figure 10. Ectopic and allelic pairing of the *lac* operator arrays in EL702C plants. (A) Percentage of loci showing ectopic pairing (untreated hemizygous nuclei) or ectopic/allelic pairing (untreated and Dex-treated homozygous nuclei). (B) Scheme of chromosome 3 (EL702C) with indicated position of used probes. (C) Sample of hemizygous nuclei showing ectopic pairing (top) or separation (bottom) of transgenic loci. (D) Sample of homozygous nuclei with ectopic pairing of both transgenic loci (top), allelic pairing of only the distal locus (middle) or separation of both loci (bottom). Nuclei were counterstained with DAPI. Bars, 3 μ m.

To to find out possible effects of *lac* operator loci on the neighboring regions, the pairing frequency of BACs F18C1 (yellow) and MGL6 (red) that flank the *lac* operator array in EL702C nuclei was analyzed by two-color FISH in wild-type ($n=153$) versus

hemizygous ($n=60$) and homozygous ($n=62$) EL702C nuclei without Dex-treatment. In addition, 61 and 59 nuclei of wild-type and homozygous EL702C after Dex-treatment were also analyzed (Figure 11).

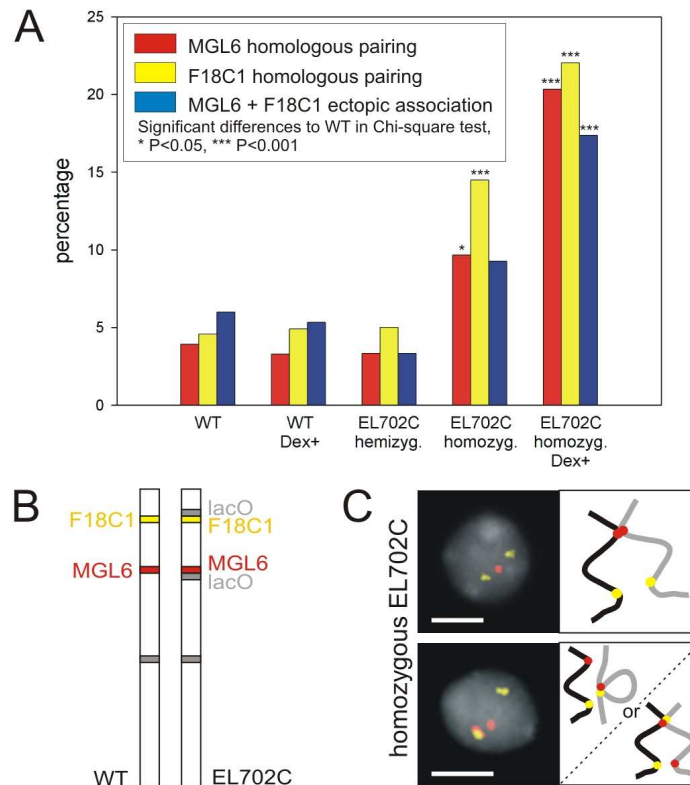


Figure 11. Homologous pairing and ectopic association of regions flanking the *lac* operator transgene. (A) Percentage of homologously paired MGL6 loci, homologously paired F18C1 loci and association between both regions in wild-type, hemizygous and homozygous EL702C nuclei without or after Dex treatment. (B) Schemes of chromosome 3 (wild-type and EL702C) showing the position of BACs MGL6 and F18C1 used for FISH. (C) Homozygous EL702C nuclei showing homologous pairing of MGL6 (top) or ectopic association intrachromosomally or between homologues (bottom). Nuclei were counterstained with DAPI. Bars, 3 μ m.

Homologous pairing of both regions as well as their heterologous association occurred without significant differences (i.e. 3%-6% per locus, Figure 11A) in wild-type and hemizygous EL702C nuclei, irrespective of Dex-treatment. In homozygous EL702C nuclei, homologous pairing (10%, $P<0.05$ for MGL6 and 14%, $P<0.001$ for F18C1) and

ectopic association (9%, $P>0.05$) occurred more often than in wild-type. A further increase of homologous pairing (20%, $P=0.032$ and 22%, $P=0.177$, respectively) as well as of ectopic association (17%, $P=0.013$; Figure 11A) was found after induction of GFP-lac repressor protein expression in homozygous EL702C nuclei (all at $P<0.001$ when compared to wild-type).

Homologous pairing of ~100 kb regions along different chromosomes of *A. thaliana* accession Col occurs on an average in about 5% of somatic nuclei (see part 3.2.4.). In wild-type nuclei, allelic pairing and ectopic association of the regions that flank the *lac* operator loci in EL702C occur with a similar frequency (3%-6% per locus). These values are also within the range predicted for random appearance of homologous pairing according to simulations based on the RSD model (see Materials and methods). The homozygous presence of the *lac* operator arrays results in a 4-fold to 10-fold higher frequency of allelic as well as of ectopic pairing of these loci compared to the average values observed for endogenous sequences in wild-type nuclei (compare values for BACs F18C1 and MGL6 in Figure 11A with those for *lac* operator arrays in Figure 10A). The high allelic pairing frequency of the transgene may exert a “dragging” effect on the flanking regions (Figure 11A). In hemizygotes, a dragging effect is not obvious because (i) pairing of the transgene is less frequent than in homozygotes and (ii) in most cases FISH signals of flanking regions are separated by those of *lac* operator loci during ectopic transgene pairing. On the basis of these data it is speculated that tandem repetitive sequences promote homologous association in Arabidopsis. Such a tendency for homologous association of tandem repeats could also be the reason for association of multiple transgene insertion loci in wheat nuclei (Abranches et al. 2000; Santos et al. 2002).

Expression of the GFP-lac repressor protein in homozygous EL702C nuclei yielded a further increase of allelic and ectopic pairing of the transgene locus by

additional 5 to 10% (Figure 10A), with a dragging effect on the flanking regions (Figure 11A). Most likely, GFP-lac repressor protein binding to the *lac* operator arrays, rather than just expression of the transgene, enforces allelic and ectopic pairing of the *lac* operator arrays. Wild-type *lac* repressor (tetramerizing form) can bind *lac* operators on different DNA molecules, tethering together loci on different chromosomes (Straight et al. 1996; Weiss and Simpson 1997). Because in this study a dimerizing mutant form of the lac repressor was used (Kato and Lam 2001), which can bind only one *lac* operator site (Robinett et al. 1996), the capability of tethering two chromosomes should be minimized in EL702C. Nevertheless, spontaneous association of GFP-lac repressor protein molecules bound to different *lac* operator loci might increase the pairing frequency. Previously, Kato and Lam (2003) reported that movement of tagged chromatin in Arabidopsis nuclei, in spite of being spatially constrained, may span $\sim 0.085\mu\text{m}/\text{min}$. Because homologous chromosome regions of ~ 100 kb are either paired or separated by less than $0.2\ \mu\text{m}$ in $\sim 20\%$ of Arabidopsis nuclei on average, it seems reasonable to assume that during the 12 h of Dex-treatment random associations of *lac* operator sites may occur and become stabilized due to aggregation of GFP-lac repressor proteins.

The pairing behavior of *lac* operator arrays is apparently not sequence specific. A similar pairing frequency as for the *lac* operator arrays was found also for the tandem repetitive transgenic hygromycin phosphotransferase (HPT) locus (composed of ~ 15 rearranged plasmid copies of together ~ 100 kb) (data of A. Probst in Pecinka et al. J. Cell Sci, *submitted*). This locus is silent within the homozygous *A. thaliana* line A (Mittelsten Scheid et al. 1991, 1998) and activated in the *mom1-1* mutant (Amedeo et al. 2000) without alteration of DNA methylation and histone modifications (Probst et al. 2003). In nuclei of line A, 30% of HPT FISH signals were paired. This value is significantly higher ($P < 0.001$) than the $\sim 5\%$ of pairing observed for various endogenous

euchromatic regions along the Arabidopsis chromosomes (Pecinka et al. 2004). However, it is not significantly different ($P>0.05$) from the allelic pairing frequency of transgenic *lac* operator arrays (34% of loci) in homozygous EL702C nuclei. In *mom1-1* nuclei, association of HPT FISH signals (21%) was still significantly higher than the average pairing frequency of Arabidopsis endogenous euchromatic regions ($P<0.001$).

Sequence-specific but more or less location-independent somatic association of multiple inserted arrays of *tet* operator and *lac* operator has been reported for budding yeast (Aragon-Alcaide and Strunnikov 2000) although this was not confirmed by FISH or in the absence of fusion protein. For the same organism, association of *tet* operator arrays was shown to depend on the expression of the *tet* repressor fusion-protein (Fuchs et al. 2002). In *Drosophila*, *lac* O arrays apparently do not necessarily enforce homologous pairing since it was possible to trace extensive separation of homologues and even of sister chromatids during premeiotic mid-G2 (Vazquez et al. 2002), although somatic pairing occurs regularly in many *Drosophila* tissues.

3.3.4. The transgenic tandem repeats co-localize more often than the flanking regions with heterochromatic chromocenters

During the FISH analysis described above, a frequent spatial association of *lac* operator loci with heterochromatic chromocenters (detected as strongly DAPI-stained regions) was noticed. Therefore the frequency of positional overlap (co-localization) of FISH signals of F18C1, MGL6 and *lac* operator probes with strongly DAPI-stained chromocenters was quantified in homozygous EL702C nuclei without ($n=41$) and after Dex-treatment ($n=31$). For comparison, the overlap of FISH signals of MGL6 and F18C1 probes with heterochromatin was monitored in 62 wild-type nuclei (Figure 12). In wild-type nuclei, chromocenters could not be clearly distinguished only on the basis of

DAPI staining. Therefore, they were marked by FISH with 180 bp centromeric repeats and 45S rDNA, the main components of heterochromatin in *Arabidopsis* (Fransz et al. 2002). While 8-14% of MGL6 and F18C1 FISH signals co-localized with heterochromatin in all types of nuclei tested, 37% of *lac* operator signals overlapped with chromocenters in untreated, and 44% in Dex-treated homozygous EL702C nuclei (both $P < 0.001$ when compared to the flanking regions). Apparently, the co-localization of *lac* operators with heterochromatin did not interfere with expression of the GFP-*lac* repressor protein in homozygous EL702C nuclei although the *lac* repressor gene is placed closely to the *lac* operator array (Figure 12).

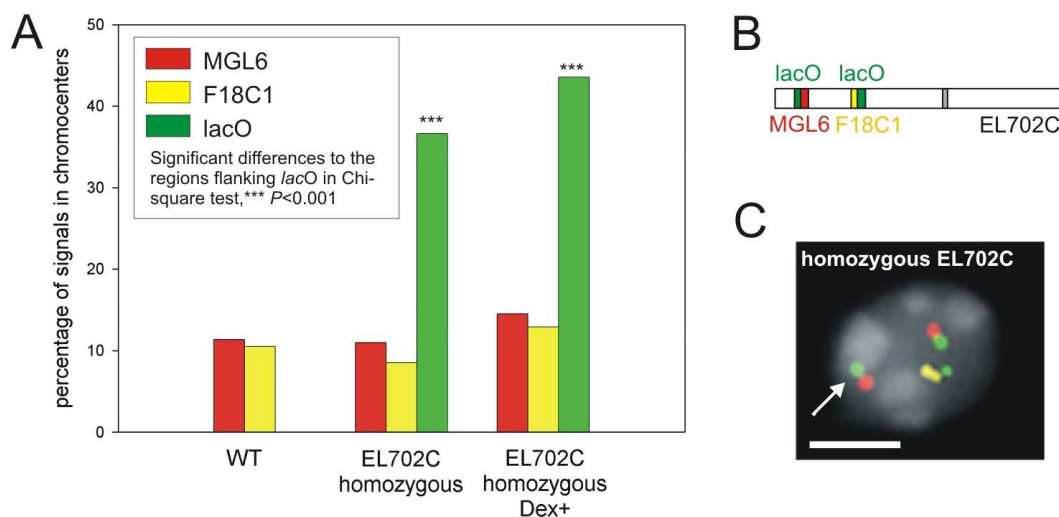


Figure 12. Association frequency of the *lac* operator arrays and of BACs F18C1 and MGL6 with heterochromatin domains. (A) The percentage of FISH signals associated with heterochromatin in nuclei of wild-type (MGL6, F18C1) and of homozygous EL702C plants without and after Dex treatment (MGL6, F18C1, *lac* operator) is shown. (B) Scheme of chromosome 3 (EL702C) with positions of the sequences used for FISH. (C) Homozygous EL702C nucleus with one distal *lac* operator FISH signal within a DAPI-intense heterochromatin chromocenter (arrow). The second one and the paired proximal *lac* operator FISH signals as well as all flanking regions are in euchromatin. The nucleus was counterstained with DAPI. Bar, 3 μ m.

In order to test whether pairing of *lac* operator loci precedes association with heterochromatin, the number of *lac* operator loci per overlap with a chromocenter was counted. Within 31 Dex-treated homozygous EL702C nuclei (harboring 124 loci), 54 loci were associated with a chromocenter, of which 14 were detected as a single locus, 24 as two, 12 as three and 4 as four paired loci suggesting that transgene pairing is not a prerequisite for association with heterochromatin.

Similar observations as to the association with heterochromatic chromocenters were made also for the transgenic HPT locus (A. Probst in Pecinka et al. 2005). Co-localization with heterochromatic chromocenters was found for 50% of HPT signals in line A and for 49% in *mom1-1* nuclei. This is significantly more ($P < 0.001$) than found for BACs MGL6 and F18C1 in wild-type. Because 60-65% of heterochromatin-associated HPT loci were not paired, homologous pairing seems not to be a prerequisite for spatial association of HPT loci with chromocenters. Hence, the association frequency of the HPT locus with heterochromatin is even higher than that observed for the *lac* operator arrays, independent of its transcriptional status and of a preceding homologous pairing. The HPT locus is clearly larger than the *lac* operator locus and becomes often visible as an intensely DAPI-stained chromocenter (Probst et al. 2003). Because the HPT locus co-localized more often than the *lac* operator locus with heterochromatin, the tendency of tandem repeats to associate with heterochromatin in Arabidopsis interphase nuclei might correlate with the size of the entire repeat containing locus.

The mechanism by which repeat sequences are targeted to chromocenters remains to be elucidated. Probably, tandem repeat loci tend to associate with each other on the basis of sequence homology but also with heterochromatic chromocenters containing other repeat sequences. This would render tandem repeats better candidates for anchoring euchromatin loops to heterochromatin according to the 'chromocenter-loop-model' (Fransz et al. 2002) than dispersed repeats such as

Emi12 elements that colocalize with chromocenters only in 1-7% of nuclei (S. Klatte and I. Schubert unpublished results).

3.3.5. Conclusions as to the local alterations of interphase chromosome arrangement caused by repetitive transgenes and fluorescent chromatin tags

Fluorescent protein mediated chromatin tagging as achieved by the *lac* operator/*lac* repressor system is useful to trace distinct chromatin domains in living eukaryotic nuclei. To interpret the data correctly, it is important to recognize influences of the tagging system on nuclear architectures of the host cells. Within an *Arabidopsis* line that carries *lac* operator/*lac* repressor/GFP transgenes, the transgene loci frequently associate with each other and with heterochromatic chromocenters. Accumulation of tagging fusion protein further enhances the association frequency. Experiments with a transgenic plant carrying another multi-copy transgene also revealed, independent of its transcriptional state, unusually high frequencies of association with each other and with heterochromatin. From these results it is concluded: (i) the *lac* operator/*lac* repressor chromatin tagging system may alter the spatial chromatin organization in the host nuclei (in particular when more than one insertion locus is present) and (ii) loci of homologous transgenic repeats associate more often with each other and with endogenous heterochromatin than average euchromatic regions.

4. Outlook

- i) In previous studies, I could show that transgenic tandem repetitive *lac* operator arrays frequently associate with each other and with heterochromatic chromocenters in Arabidopsis nuclei. The original tagged line was crossed with Arabidopsis mutants (*ddm1* and *met1*) showing reduced levels of DNA and histone methylation and altered chromatin organization in interphase nuclei (Soppe et al. 2002) within the group of E. Lam. Future studies using these tagged mutant lines will show whether the global changes in DNA methylation and histone modifications have an impact on homologous pairing and heterologous association of interstitial tandem repeats.
- ii) Whole-mount FISH experiments on Arabidopsis root meristematic tissues will show whether the CT arrangement in mitotically active cells differs from that observed in differentiated tissues. Nuclei of meristematic cells have a prominent phenotype (spheric shape; large nucleolus comprising at least 50-60% of nuclear volume and chromatin occupying only relatively thin layer adjacent to the nuclear periphery) and thus differ significantly from previously analyzed Arabidopsis nuclei. Therefore, new SCD model simulations of random CT arrangement in nuclei of meristematic cells will be performed.
- iii) The seeds of flowering plants contain two fertilization products: the diploid embryo and triploid endosperm. The embryo results from a fusion between the maternal genome of the egg and the paternal genome of the sperm. The endosperm is a product of fusion between one paternal genome of the sperm and the two maternal genomes of the (homo-diploid) central cell. The ploidy ratio of two maternal to one paternal genome in the endosperm is critical for normal seed development. So far, the role of higher-order chromatin structure in endosperm

nuclei, and in particular, the arrangement of the parental genomes, have not been investigated. Using CP, it is aimed to determine whether the parental genomes in *Arabidopsis* endosperm nuclei possess a non-random arrangement and/or a specific topology that could underlie the parent-of-origin effects observed during seed development.

- iv) (Peri)centromeric and telomeric regions associate more frequently than interstitial euchromatic chromosome regions in *Arabidopsis* nuclei. Based on this observation, it is assumed that interstitial regions should be involved less frequently than chromocenters and chromosome termini in spontaneous and induced homologous exchange aberrations. During the first post-treatment mitosis after mutagen exposure, multicolor CP should allow to identify the chromosomes involved in exchange aberrations. If *Arabidopsis* chromosome regions containing tandemly repeated sequences are preferentially involved in mutagen-induced structural chromosome aberrations as observed for other organisms (Schubert et al. 1994, 2004), the breakpoints of exchange aberrations in the first post-treatment mitoses should predominantly occur within pericentromeric or NOR regions detectable by size and composition of anaphase bridges and/or acentric fragments after multicolor CP.
- v) Comparative CP to other species of the *Brassicaceae* family is now feasible (Lysak et al. 2003). This method is utilizing *A. thaliana* chromosome specific painting probes arranged according to comparative genetic maps of *Arabidopsis lyrata* and *Capsella rubella* (Schmidt et al. 2004; Kuittinen et al. 2004). Studies on interphase nuclei of related *Brassicaceae* species, will show whether a chromosomal constitution different from that of *A. thaliana* results in a different CT arrangement. The experimental results will be compared to corresponding SCD model predictions for random CT arrangement.

5. Summary

I. Establishing of chromosome painting in *Arabidopsis thaliana* and detection of chromosome rearrangements

Painting experiments with the complete set of BACs from the chromosome 4 tiling path resulted in cross-hybridization signals on other chromosomes (Lysak et al. 2001). Therefore, individual BACs were analyzed for the presence of repetitive DNA sequences in TIGR database and by Dot Blot hybridization. Clones containing >5% of mobile elements in TIGR database or yielding strong hybridization signals on Dot Blot were omitted from the painting probes. From 1,585 tested BACs, 77% were considered as suitable for CP.

Confirmed CP probes allow visualization of chromosome rearrangements. For the transgenic *Arabidopsis* line T665-IST, sequencing of the T-DNA insertion site suggested a translocation between the top arm of chromosome 3 and the bottom arm of chromosome 5 (Aufsatz et al. 2002). Using CP, the predicted rearrangement could be verified and the position of the chromosome 5 bottom arm terminus that was unknown for T665-IST was found on the top-arm of chromosome 3, providing evidence for a reciprocal translocation between both chromosomes. Furthermore, a previously not suspected inversion between two T-DNA insertion sites (4.2 Mbp apart from each other) on the top arm of chromosome 3 was detected by CP in the *Arabidopsis* line EL702C (Kato and Lam 2003).

II. Arrangement of interphase CTs and homologous pairing in somatic nuclei of *A. thaliana*

Using chromosome specific painting probes, arrangement and potential dynamics of Arabidopsis CTs were studied in 2C, 4C and 8C nuclei from roots and leaves. Individual CTs were found to be frequently associated. However, this arrangement corresponds to the computer model prediction for random CT arrangement and is due to the low number of Arabidopsis chromosomes ($2n=10$). Only the homologues of the NOR-bearing chromosomes 2 and 4, associate more frequently than expected at random. This is apparently because of frequent attachment of NORs to a single nucleolus (in >90% of Arabidopsis nuclei), which mediates association of NOR-bearing arms and of entire homologues. This arrangement was consistently found in all investigated types of nuclei. Furthermore, the relative position of a gene (*FWA*) within its chromosome territory does not obviously depend on its transcriptional state.

Single-point homologous pairing occurs on average in 4.9% of somatic nuclei, i.e. not significantly more than expected at random (5.9-7.8%). Only in 0.2% of nuclei, two segments at distant chromosomal positions were found to pair simultaneously. No significant differences as to the frequency of positional homologous pairing were observed in Arabidopsis mutants with an increased frequency of somatic homologous recombination. This suggests that the increase in recombination frequency is rather due to more intensified search for homology after spontaneous as well as induced DNA damage than to a generally increased level of homologous associations.

Thus Arabidopsis differs from *Drosophila* (characterized by regular somatic pairing of homologues) and shows that similarity in genome size, sequence organization and chromosome number does not necessarily cause an identical arrangement of interphase chromosomes.

III. Alteration of the local interphase chromosome arrangement by tandem repetitive transgenes and fluorescent chromatin tags

The lac operator/GFP-lac repressor tagging system is a powerful tool to study chromatin dynamics *in vivo*. However, the results as to the arrangement of interphase chromosomes achieved with this system have to be considered cautiously. In many Arabidopsis nuclei lac operator arrays do not reflect the spatial organization at the integration loci under wild-type condition and may lead to invalid conclusions as to positional homologous pairing frequencies (Esch et al. 2003). This problem could become significant especially when homozygous or multiple insertions of repetitive arrays are present. The main reason for the increase in allelic and ectopic association frequency of the lac operator arrays (compared to the flanking sequences under wild-type condition) is most likely the repetitive nature of the transgene construct. The similar behavior of the HPT locus further supports the idea that in *A. thaliana* the tandem repetitive nature of a transgene locus might be responsible for an increased allelic and ectopic pairing frequency of transgenic sequences as well as for an increased co-localization frequency with endogenous heterochromatin. GFP-lac repressor protein molecules that tag the lac operator arrays may further enhance the frequency of homologous pairing of the operator repeats, most likely via aggregation of lac repressor molecules bound to the different lac operator arrays in close vicinity.

6. Zusammenfassung

I. Etablierung des Chromosomenpaintings für *Arabidopsis thaliana* und Nachweis von Chromosomenumbauten

Painting-Experimente mit einem Satz künstlicher Bakterienchromosomen (BACs), die das gesamte Chromosom 4 abdecken, ergaben Hybridisierungssignale auch auf den anderen Chromosomen (Lysak et al. 2001). Deshalb wurden alle verfügbaren BACs für die übrigen 4 Chromosomen anhand von Datenbank-Annotationen (TIGR) und mittels Dot-Blot-Hybridisierung mit genomischer DNA auf Anwesenheit von repetitiven Sequenzen überprüft. Klone, die mehr als 5% mobile Elemente oder starke Hybridisierungssignale mit genomischer DNA aufwiesen, wurden nicht in die Painting-Proben einbezogen. Von 1585 BACs wurden 77% als für das Painting geeignet gefunden.

Selektierte Painting-Proben ermöglichten den Nachweis von strukturellen Chromosomenaberrationen. Die Sequenzierung eines T-DNA-Insertionsortes in der transgenen *Arabidopsis*-Linie T655-IST liess eine Translokation zwischen dem kurzen Arm von Chromosom 3 und dem langen Arm von Chromosom 5 vermuten (Aufsatz et al. 2002). Durch Chromosomenpainting konnte diese Annahme verifiziert werden. Weiterhin konnte eine vordem nicht vermutete Inversion zwischen zwei 4,2 Mb voneinander entfernten T-DNA-Insertionsorten im kurzen Arm von Chromosom 3 der Linie EL702C (Kato & Lam 2003) mittels geeigneter Painting-Proben *in situ* nachgewiesen werden.

II. Anordnung von Interphase-Chromosomenterritorien und homologe Paarung in somatischen Zellkernen von *A. thaliana*

Mittels chromosomenspezifischer Painting-Proben wurden die Anordnung und die potentielle Dynamik von Chromosomenterritorien in 2C-, 4C- und 8C-Kernen

unterschiedlicher Form (kugelig, spindelförmig, stabförmig) aus Wurzeln und Blättern von *A. thaliana* untersucht. Individuelle Chromosomenterritorien waren größenabhängig in beliebigen homo- und heterologen Kombinationen (x – y% der Kerne) miteinander positionell assoziiert. Diese Anordnung entsprach der Vorhersage durch Computersimulationen gemäß einer zufälligen Chromosomenanordnung und beruht auf der geringen Chromosomenzahl von *A. thaliana* ($2n = 10$). Lediglich die Homologen der NOR-tragenden Chromosomen 2 und 4 waren häufiger assoziiert als zufallsgemäß erwartet. Dieser Befund beruht wahrscheinlich darauf, dass in >90% der untersuchten Kerne alle Nukleolusorganisatoren mit nur einem Nukleolus in einer Weise vergesellschaftet waren, die die Assoziation von NOR-tragenden Armen sowie vollständiger homologer NOR-Chromosomen bedingte. Diese Anordnung wurde in allen untersuchten Kerntypen gefunden.

Am Beispiel des Blütengens FWA konnte gezeigt werden, dass die relative Position eines Gens innerhalb oder außerhalb des entsprechenden durch Painting markierten Territoriums nicht zwingend von der Transkriptionsaktivität abhängt. Punktuelle Homologenpaarung tritt an unterschiedlichen chromosomalen Positionen durchschnittlich in 4,9% der Zellkerne auf, d.h. nicht häufiger als zufallsgemäß (in 5,9 – 7,8 % der Kerne) erwartet.

Auch in Mutanten mit signifikant erhöhter Frequenz an somatischen homologen Rekombinationsereignissen bleibt die punktuelle Paarungsfrequenz unverändert. Wahrscheinlich basiert die erhöhte Rekombinationsfrequenz eher auf einer intensiveren "Homologie-Suche" als auf häufigerer Homologenpaarung.

Der Unterschied zu den an *Drosophila* erhobenen Befunden (reguläre somatische Homologenpaarung) zeigt, dass Ähnlichkeiten hinsichtlich Genomgröße, Sequenzorganisation und Chromosomenzahl nicht notwendigerweise eine gleiche Anordnung der Interphasechromosomen bedingen.

III. Lokale Veränderungen der Chromosomenanordnung durch tandem-repetitive Transgene und fluoreszierende 'Chromatin-tags'

Das Lac-Operator/GFP-Lac-Repressor-System ist ein geeignetes Werkzeug zum Studium der Chromatindynamik *in vivo*. Jedoch sind die entsprechenden Ergebnisse mit Vorsicht zu betrachten, da es sich um künstlich geschaffene Loci mit z.T. unnatürlichen Proteinkonzentrationen handelt. In vielen Arabidopsiskernen spiegelt die Anordnung der Lac-Operator-Repeats daher auch nicht die räumliche Organisation der entsprechenden Loci unter Wildtypbedingungen wider und kann zu falschen Schlußfolgerungen hinsichtlich der punktuellen Homologenpaarung führen (Esch et al. 2003). Dies ist vor allem dann der Fall, wenn homozygote oder multiple Insertionen von Tandem Repeats vorliegen. Die wesentliche Ursache für die erhöhte Frequenz allerer und ektopischer Paarung der Lac-Operator-Repeats im Vergleich zu flankierenden Sequenzen unter Wildtypbedingungen liegt höchstwahrscheinlich in der repetitiven Struktur des transgenen Konstruktes. Ein ähnliches Verhalten des HPT-Locus unterstützt die Annahme, dass in Arabidopsis die tandemrepetitive Natur von Transgen-Loci für eine erhöhte Frequenz der homologen Paarung solcher Loci untereinander sowie für eine häufigere Assoziation mit endogenem Heterochromatin verantwortlich ist.

GFP-Lac-Repressormoleküle bewirken wahrscheinlich eine zusätzliche Erhöhung der Homologen-Paarungsfrequenz von Lac-Operator-Repeats durch Aggregation von an unterschiedliche aber benachbarte Repeats gebundenen Repressormolekülen.

7. Literature

Abranches R., Beven A.F., Aragón-Alcaide L., and Shaw P.J. (1998). Transcriptional sites are not correlated with chromosome territories in wheat nuclei. *J Cell Biol.* *143*, 5-12.

Abranches R., Santos A.P., Wegel E., Williams S., Castilho A., Christou P., Shaw P., and Stoger E. (2000). Widely separated multiple transgene integration sites in wheat chromosomes are brought together at interphase. *Plant J* *24*, 713-723.

Amedeo P., Habu Y., Afsar K., Mittelsten Scheid O., and Paszkowski J. (2000). Disruption of the plant gene MOM releases transcriptional silencing of methylated genes. *Nature* *405*, 203-206.

Aragon-Alcaide L. and Strunnikov A.V. (2000). Functional dissection of in vivo interchromosome association in *Saccharomyces cerevisiae*. *Nat. Cell Biol.* *2*, 812-818.

Aragón-Alcaide L., Reader S., Beven A., Shaw P., Miller T., and Moore G. (1997). Association of homologous chromosomes during floral development. *Curr. Biol.* *7*, 905-908.

Aufsatz W., Mette M.F., van der Winden J., Matzke A.J.M., and Matzke M. (2002). RNA-directed DNA methylation in *Arabidopsis*. *Proc. Natl. Acad. Sci. USA* *99*, 16499-16506.

Belmont A.S., Li G., Sudlow G., and Robinett C. (1999). Visualization of large-scale chromatin structure and dynamics using the lac operator/lac repressor reporter system. *Methods Cell Biol.* *58*, 203-222.

Bennett M.D., Leitch I., Price J.H., and Johnston S.J. (2003). Comparisons with *Caenorhabditis* (100 Mb) and *Drosophila* (175 Mb) using flow cytometry show genome size in *Arabidopsis* to be 157 Mb and thus 25 % larger than the *Arabidopsis* Genome Initiative estimate of 125 Mb. *Ann. Bot.* *91*, 1-11.

Blennow E. (2004). Reverse painting highlights the origin of chromosome aberrations. *Chromosome Res.* *12*, 25-33.

Bickmore W.A. and Chubb J.R. (2003). Chromosome position: Now, where was I? *Curr. Biol.* *13*, R357-R359.

- Boivin K., Acarcan A., Mbulu R.-S., Clarenz O., and Schmidt R. (2004). The Arabidopsis genome sequence as a tool for genome analysis in Brassicaceae. A comparison of the Arabidopsis and *Capsella rubella* genomes. *Plant Physiol.* *135*, 735-744.
- Bridger J.M., Boyle S., Kill I.R., and Bickmore W.A. (2000). Re-modelling of nuclear architecture in quiescent and senescent human fibroblasts. *Curr. Biol.* *10*, 149-152.
- Burgess S.M., Kleckner N., and Weiner B.M. (1999). Somatic pairing of homologs in budding yeast: existence and modulation. *Genes & Dev.* *13*, 1627-1641.
- Chandler V.L. and Stam M. (2004). Chromatin conversations: mechanisms and implications of paramutation. *Nat. Rev. Genet.* *5*, 532-544.
- Chandley A.C., Speed R.M., and Leitch A.R. (1996). Different distributions of homologous chromosomes in adult human Sertoli cells and in lymphocytes signify nuclear differentiation. *J Cell Sci.* *109*, 773-776.
- Cornforth M.N., Greulich-Bode K.M., Loucas B.D., Arsuaga J., Vázquez M., Sachs R.K., Brückner M., Molls M., Hahnfeldt P., Hlatky L., and Brenner D.J. (2002). Chromosomes are predominantly located randomly with respect to each other in interphase human cells. *J. Cell Biol.* *159*, 237-244.
- Cremer M., von Hase J., Volm T., Brero A., Kreth G., Walter J., Fischer C., Solovei I., Cremer C., and Cremer T. (2001). Non-random radial higher-order chromatin arrangements in nuclei of diploid human cells. *Chromosome Res.* *9*, 514-567.
- Cremer T., Popp S., Emmerich P., Lichter P., and Cremer C. (1990). Rapid metaphase and interphase detection of radiation-induced chromosome aberrations in human lymphocytes by chromosomal suppression in situ hybridization. *Cytometry* *11*, 110-118.
- Cremer T. and Cremer C. (2001). Chromosome territories, Nuclear architecture and Gene regulation in Mammalian cells. *Nat. Rev. Genet.* *2*, 292-301.
- Csink A.K. and Henikoff S. (1998). Large-scale chromosomal movements during interphase progression in *Drosophila*. *J. Cell Biol.* *143*, 13-22.
- Dong F. and Jiang J. (1998). Non-Rabl patterns of centromere and telomere distribution in the interphase nuclei of plant cells. *Chromosome Res.* *6*, 551-558.
- Duncan I.W. (2002). Transvection effects in *Drosophila*. *Annu. Rev. Genet.* *36*, 521-556.

- Esch J.J., Chen M., Sanders M., Hillestad M., Ndkium S., Idelkope B., Neizer J., and Marks M.D. (2003). A contradictory GLABRA3 allele helps define gene interactions controlling trichome development in *Arabidopsis*. *Development* 130, 5885-5894.
- Ferguson-Smith M.A. (1997). Genetic analysis by chromosome sorting and painting: phylogenetic and diagnostic applications. *Eur. J Hum. Genet.* 5, 253-265.
- Fransz P., Armstrong S., Alonso-Blanco C., Fischer T.C., Torres-Ruiz R.A., and Jones G. (1998). Cytogenetics for the model system *Arabidopsis thaliana*. *Plant J* 13, 867-876.
- Fransz P.F., Armstrong S., de Jong J.H., Parnell D., van Drunen C., Dean C., Zabel P., Bisseling T., and Jones G.H. (2000). Integrated cytogenetic map of chromosome arm 4S of *A. thaliana*: Structural organization of heterochromatic knob and centromere region. *Cell* 100, 367-376.
- Fransz P., de Jong J.H., Lysak M.A., Ruffini Castiglione M., and Schubert I. (2002). Interphase chromosomes in *Arabidopsis* are organized as well defined chromosomers from which euchromatin loops emanate. *Proc. Natl. Acad. Sci. USA* 99, 14584-14589.
- Fuchs J., Lorenz A., and Loidl J. (2002). Chromosome associations in budding yeast caused by integrated tandemly repeated transgenes. *J Cell Sci.* 115, 1213-1220.
- Fung J.C., Marshall W.F., Dernburg A., Agard D.A., and Sedat J.W. (1998). Homologous chromosome pairing in *Drosophila melanogaster* proceeds through multiple independent initiations. *J. Cell Biol.* 141, 5-20.
- Gasser S.M. (2002). Visualizing chromatin dynamics in interphase nuclei. *Science* 296, 1412-1416.
- Gerlich D., Beaudouin J., Kalbfuss B., Daigle N., Eils R., and Ellenberg J. (2003). Chromosome positioning in live mammalian cells. *Cell* 112, 751-764.
- Gunawardena S. and Rykowski, M.C. (2000). Direct evidence for interphase chromosome movement during the mid-blastula transition in *Drosophila*. *Curr.Biol.* 10, 285-288.
- Habermann F.A., Cremer M., Walter J., Kreth G., von Hase J., Bauer K., Wienberg J., Cremer C., Cremer T., and Solovei I. (2001). Arrangements of macro- and microchromosomes in chicken cells. *Chromosome Res.* 9, 569-584.
- Heitz E. (1928). Heterochromatin der Moose I. *Jahrb. Wiss. Bot.* 69, 762-818.
- Henegariu O., Bray-Ward P., and Ward D.C. (2000). Custom fluorescent-nucleotide synthesis as an alternative method for nucleic acid labeling. *Nat. Biotech.* 18, 345-348.

- Hiraoka Y., Dernburg A.F., Parmelee S.J., Rykowski M.C., and Agard D.A. (1993). The Onset of homologous chromosome pairing during *Drosophila melanogaster* embryogenesis. *J. Cell Biol.* *120*, 591-600.
- Hobza R., Lengerova M., Cernohorska H., Rubes J., and Vyskot B. (2004). FAST-FISH with laser beam microdissected DOP-PCR probe distinguishes the sex chromosomes of *Silene latifolia*. *Chromosome Res.* *12*, 245-250.
- Houben A., Kynast R.G., Heim U., Hermann H., Jones R.N., and Forster J.W. (1996). Molecular cytogenetic characterization of the terminal heterochromatic segment of the B-chromosome of rye (*Secale cereale*). *Chromosoma* *105*, 97-103.
- Kato N. and Lam E. (2001). detection of chromosomes tagged with green fluorescent protein in live *Arabidopsis thaliana* plants. *Genome Biol.* *2*, 0045.1-0045.10.
- Kato N. and Lam E. (2003). Chromatin of endoreduplicated pavement cells has greater range of movement than that of diploid guard cells in *Arabidopsis thaliana*. *J Cell Sci.* *116*, 2195-2201.
- Kato A., Lamb J.C., and Birchler J.A. (2004). Chromosome painting using repetitive DNA sequences as probes for somatic chromosome identification in maize. *Proc. Natl. Acad. Sci. USA* *101*, 13554-13559.
- Kozubek S., Lukasova E., Jirsova P., Koutna I., Kozubek M., Ganova A., Bartova E., Falk M., and Pasekova R. (2002). 3D Structure of the human genome: order in randomness. *Chromosoma* *111*, 321-331.
- Kreth G., Finsterle J., von Hase J., Cremer M., and Cremer C. (2004). Radial Arrangement of Chromosome Territories in Human Cell Nuclei: A Computer Model Approach Based on Gene Density Indicates a Probabilistic Global Positioning Code. *Biophys. J* *86*, 2803-2812.
- Kuittinen H., de Haan A.A., Vogl C., Oikarinen S., Leppälä J., Koch M., Mitchell-Olds T., Langley C.H., and Savolainen O. (2004). Comparing the linkage maps of the close relatives *Arabidopsis lyrata* and *A. thaliana*. *Genetics* *168*, 1575-1584.
- Lam E., Kato N., and Watanabe K. (2004). Visualizing chromosome structure/organization. *Ann Rev Plant Biol.* *55*, 537-554.
- Langer S., Kraus J., Jentsch I., and Speicher M.R. (2004). Multicolor chromosome painting in diagnostic and research applications. *Chromosome Res.* *12*, 15-23.

- Laufs P., Autran D., and Traas J. (1999). A chromosomal paracentric inversion associated with T-DNA integration in *Arabidopsis*. *Plant J* 18, 131-139.
- Lichter P., Cremer T., Borden J., Manuelidis L., and Ward D.C. (1988). Delineation of individual human chromosomes in metaphase and interphase cells by in situ suppression hybridization using recombinant DNA libraries. *Hum. Genet.* 80, 224-234.
- Lorenz A., Fuchs J., Bürger R., and Loidl J. (2003). Chromosome pairing does not contribute to nuclear architecture in vegetative yeast cells. *Eucaryotic Cell* 2, 856-866.
- Lysak M.A., Fransz P.F., Ali H.B.M., and Schubert I. (2001). Chromosome painting in *Arabidopsis thaliana*. *Plant J* 28, 689-697.
- Lysak M.A., Pecinka A., and Schubert I. (2003). Recent progress in chromosome painting of *Arabidopsis* and related species. *Chromosome Res.* 11, 195-204.
- Lysak M.A., Koch M., Pecinka A., and Schubert I. (2005). Chromosome triplication found across the tribe *Brassicaceae*. *Genome Res. in revision*.
- Mahy N.L., Perry P.E., Gilchrist S., Baldock R., and Bickmore W.A. (2002). Spatial organisation of active and inactive genes and noncoding DNA with chromosome territories. *J. Cell Biol.* 157, 579-589.
- Mahy N.L., Perry P.E., and Bickmore W.A. (2002). Gene density and transcription influence the localization of chromatin outside of chromosome territories detectable by FISH. *J. Cell Biol.* 159, 753-763.
- Marshall R. and Obe G. (1998). Application of chromosome painting to clastogenicity testing in vitro. *Environ. Mol. Mutagen.* 32, 212-222.
- Martínez-Pérez E., Shaw P., and Moore G. (2001). Polyploidy induces centromere association. *J. Cell Biol.* 148, 233-238.
- Martínez-Zapater J.M., Estelle M.A., and Somerville C.R. (1986). A highly repeated DNA sequence in *Arabidopsis thaliana*. *Mol. Gen. Genet.* 204, 417-423.
- Matzke A.J.M., van der Winden J., and Matzke M. (2003). Tetracycline operator/repressor system to visualize fluorescence-tagged T-DNAs in interphase nuclei of *Arabidopsis*. *Plant Mol. Biol. Rep.* 21, 9-19.
- McKee B.D. (2004). Homologous pairing and chromosome dynamics in meiosis and mitosis. *Biochim. Biophys. Acta* 1677, 165-180.

- Metropolis N., Rosenbluth A.W., Rosenbluth M.N., Teller A.H., and Teller E. (1953) Equation of state calculations by fast computing machines. *J Chem. Phys.* *21*, 1087-1092.
- Mittelsten Scheid O., Paszkowski J., and Potrykus I. (1991). Reversible inactivation of a transgene in *Arabidopsis thaliana*. *Mol. Gen. Genet.* *228*, 104-112.
- Mittelsten Scheid O., Afsar K., and Paszkowski J. (1998). Release of epigenetic gene silencing by trans-acting mutations in *Arabidopsis*. *Proc. Natl. Acad. Sci. USA* *95*, 632-637.
- Molinier J., Ries G., Bonhoeffler S., and Hohn B. (2004). Interchromatid and interhomolog recombination in *Arabidopsis thaliana*. *Plant Cell* *16*, 342-352.
- Nabeshima K., Nakagawa T., Straight A.F., Murray A., Chikashige Y., Yamashita Y.M., Hiraoka Y., and Yanagida M. (1998). Dynamics of centromeres during metaphase-anaphase transition in fission yeast: Dis1 is implicated in force balance in metaphase bipolar spindle. *Mol. Biol. Cell* *9*, 3211-3225.
- Nagele R.G., Freeman T., McMorrow L., Thomson Z., Kitson-Wind K., and Lee H.-Y. (1999). Chromosomes exhibit preferential positioning in nuclei of quiescent human cells. *J Cell Sci.* *112*, 525-535.
- Natarajan A.T., Vyas R.C., Darroudi F., and Vermeulen S. (1992). Frequencies of X-ray-induced chromosome translocations in human peripheral lymphocytes as detected by in situ hybridization using chromosome specific libraries. *Int. J. Radiat. Biol.* *61*, 199-203.
- Parada L.A. and Misteli T. (2002). Chromosome positioning in the interphase nucleus. *Trends in Cell Biol.* *12*, 425-432.
- Parada L.A., Roix J.J., and Misteli T. (2003). An uncertainty principle in chromosome positioning. *Trends in Cell Biol.* *13*, 393-396.
- Pecinka A., Schubert V., Meister A., Kreth G., Klatte M., Lysak M.A., Fuchs J., and Schubert I. (2004). Chromosome territory arrangement and homologous pairing in nuclei of *Arabidopsis thaliana* are predominantly random except for NOR-bearing chromosomes. *Chromosoma* *113*, 258-269.
- Pecinka A., Kato N., Meister A., Probst A.V., Schubert I., and Lam E. (2005). Tandem repetitive transgenes and fluorescent chromatin tags alter the local interphase chromosome arrangement in *Arabidopsis thaliana*. *J Cell Sci.* submitted.

- Pinkel D., Landegent J., Collins C., Fuscoe J., Seagraves R., Lucas J., and Gray J. (1988). Fluorescence in situ hybridization with human chromosome-specific libraries: Detection of trisomy 21 and translocations of chromosome 4. *Proc. Natl. Acad. Sci. USA* 85, 9138-9142.
- Prieto P., Santos A.P., Moore G., and Shaw P. (2004). Chromosomes associate premeiotically and in xylem vessel cells via their telomeres and centromeres in diploid rice (*Oryza sativa*). *Chromosoma* 112, 300-307.
- Probst A.V., Franz P., Paszkowski J., and Mittelsten Scheid O. (2003). Two means of transcriptional reactivation within heterochromatin. *Plant J* 33, 743-749.
- Rabl C. (1885). Über Zelltheilung. *Morphol Jahrbuch* 10, 214-330.
- Ried T., Schrock E., Ning Y., and Wienberg J. (1998). Chromosome painting: a useful art. *Hum. Mol. Genet.* 7, 1619-1626.
- Rieger R., Michaelis A., Schubert I., and Meister A. (1973). Somatic interphase pairing of Vicia chromosomes as inferred from the hom/het ration of induced chromatid interchanges. *Mutation Res.* 20, 295-298.
- Robinett C.C., Straight A., Li G., Willhelm C., Sudlow G., Murray A., and Belmont A.S. (1996). In vivo localization of DNA sequences and visualization of large-scale chromatin organization using lac operator/repressor recognition. *J. Cell Biol.* 135, 1685-1700.
- Sambrook J. and Russell D.W. (2001). *Molecular cloning: a laboratory manual* 3rd edition Vol 1. Cold Spring Harbor Laboratory Press, Cold Spring Harbor.
- Santos A.P., Abranches R., Stoger E., Beven A., Viegas W., and Shaw P.J. (2002). The architecture of interphase chromosomes and gene positioning are altered by changes in DNA methylation and histone acetylation. *J Cell Sci.* 115, 4597-4605.
- Scherthan H., Loidl J., Schuster T., and Schweizer D. (1992). Meiotic chromosome condensation and pairing in *Saccharomyces-cerevisiae* studied by chromosome painting. *Chromosoma* 101, 590-595.
- Scholl R.L., May S.T., and Ware D.H. (2000). Seed and molecular resources for Arabidopsis. *Plant Physiol.* 124, 1477-1480.
- Schubert I., Rieger R., Fuchs J., and Pich U. (1994). Sequence organization and the mechanism of interstitial deletion clustering in a plant genome (*Vicia faba*). *Mutat. Res.* 325:1-5.

- Schubert I., Shi F., Fuchs J., and Endo T.R. (1998). An efficient screening for terminal deletions and translocations of barley chromosomes added to common wheat. *Plant J* *14*, 489-495.
- Schubert I., Fransz P.F., Fuchs J., and de Jong J.H. (2001). Chromosome painting in plants. *Methods Cell Sci.* *23*, 57-69.
- Schubert I., Pecinka A., Meister A., Schubert V., Klatte M., and Jovtchev G. (2004). DNA damage processing and aberration formation in plants. *Cytogenet Genome Res* *104*, 104-108.
- Schwarzacher T., Leitch A.R., Bennett M.D., and Heslop-Harrison J.S. (1989). In situ localization of parental genomes in a wide hybrid. *Ann. Bot.* *64*, 315-324.
- Schwarzacher T., Anamthawat-Jonsson K., Harrison G.E., Islam A.K.M.R., Jia J.Z., King I.P., Leitch A.R., Miller T.E., Reader S.M., Rogers W.J., Shi M., and Heslop-Harrison J.S. (1992). Genomic in situ hybridization to identify alien chromosomes and chromosome segments in wheat. *Theor. Appl. Genet.* *84*, 778-786.
- Shibata F., Hizume M., and Kuroki Y. (1999). Chromosome painting of Y chromosomes and isolation of a Y chromosomespecific repetitive sequence in the dioecious plant *Rumex acetosa*. *Chromosoma* *108*, 266-270.
- Stam M. and Mittelsten Scheid O. (2005). Paramutation: leaving a lasting impression. *Trends in Genetics*, *submitted*.
- Soppe W., Jacobsen S.E., Alonso-Blanco C., Jackson J.P., Kakutani T., Koornneef M., and Peeters A.J.M. (2000). The late flowering phenotype of *fwa* mutants is caused by gain-of-function epigenetic alleles of a homeodomain gene. *Molecular Cell* *6*, 791-802.
- Straight A.F., Belmont A.S., Robinett C.C., and Murray A.W. (1996). GFP tagging of budding yeast chromosomes reveals that protein-protein interactions can mediate sister chromatid cohesion. *Curr. Biol.* *6*, 1599-1608.
- Svartman M., Stone G., Page J.E., and Stanyon R. (2004). A chromosome painting test of the basal eutherian karyotype. *Chromosome Res.* *12*, 45-53.
- Tanabe H., Müller S., Neusser M., von Hase J., Calcagno E., Cremer M., Solovei I., Cremer C., and Cremer T. (2002). Evolutionary conservation of chromosome territory arrangements in cell nuclei from higher primates. *Proc. Natl. Acad. Sci. USA* *99*, 4424-4429.
- The Arabidopsis Genome Initiative (2000). Analysis of the genome sequence of the flowering plant *Arabidopsis thaliana*. *Nature* *408*, 796-815.

- Tsukamoto T., Hashiguchi N., Janicki S.M., Tumber T., Belmont A.S., and Spector, D.L. (2000). Visualization of gene activity in living cells. *Nat. Cell Biol.* 2, 871-878.
- Vazquez J., Belmont A.S., and Sedat J.W. (2002). The dynamics of homologous chromosome pairing during male *Drosophila* meiosis. *Curr. Biol.* 12, 1473-1483.
- Volpi E.V., Chevret E., Jones T., Vatcheva R., Williamson J., Beck S., Campbell R.D., Goldsworthy M., Powis S.H., Ragoussis J., Trowsdale J., and Sheer D. (2000). Large-scale chromatin organization of the major histocompatibility complex and other regions of human chromosome 6 and its response to interferon in interphase nuclei. *J. Cell Sci.* 113, 1565-1576.
- Vongs A., Kakutani T., Martienssen R.A., and Richards E.J. (1993). *Arabidopsis-thaliana* DNA methylation mutants. *Science* 260, 1926-1928.
- Walter J., Schmelleh L., Cremer M., Tashiro S., and Cremer T. (2003). Chromosome order in HeLa cells changes during mitosis and early G1, but is stably maintained during subsequent interphase stages. *J. Cell Biol.* 160, 685-697.
- Weiss K. and Simpson R.T. (1997). Cell type-specific chromatin organization of the region that governs directionality of yeast mating type switching. *Embo J.* 16, 4352-60.
- Williams R.R.E. and Fisher A.G. (2003). Chromosomes, positions please! *Nat. Cell Biol.* 5, 338-390.
- West C.E., Waterworth W.M., Sunderland P.A., and Bray C.M. (2004). *Arabidopsis* DNA double-strand break repair pathways. *Biochem. Soc. Transactions* 32, 964-966.
- Zink D., Cremer T., Saffrich R., Fischer R., Trendelenburg M.F., Ansorge W., and Stelzer E.H.K. (1998). Structure and dynamics of human interphase chromosome territories in vivo. *Hum. Genet.* 102, 241-251.

Publications in connection with the submitted dissertation

Lysak M.A., **Pecinka A.**, and Schubert I. (2003). Recent progress in chromosome painting of *Arabidopsis* and related species. *Chromosome Res.* *11*, 195-20.

Pecinka A., Schubert V., Meister A., Kreth G., Klatte M., Lysak M. A., Fuchs J., and Schubert I. (2004). Chromosome territory arrangement and homologous pairing in nuclei of *Arabidopsis thaliana* are predominantly random except for NOR-bearing chromosomes. *Chromosoma* *113*, 258-269.

Pecinka A., Kato N., Meister A., Probst A.V., Schubert I., and Lam E. (2005). Tandem repetitive transgenes and fluorescent chromatin tags alter the local interphase chromosome arrangement in *Arabidopsis thaliana*. *J Cell Sci.* *submitted*.

Declaration about the personal contribution to the manuscripts forming the basis of the dissertation

The part '**Fluorescence in situ hybridization (FISH) for chromosome painting**' is based on the work published in articles Lysak et al. (2003) *Chromosome Res.* *11*, 195-20; Pecinka et al. (2004) *Chromosoma* *113*, 258-269; and Pecinka et al. *J. Cell Sci.*, *submitted*. From the work published in the first paper, I have performed dot blot and CP experiments for development of painting probes for chromosomes 1 and 2 and identified misaligned BACs from the top-arm of chromosome 2. Later on, I have selected by Dot Blot hybridization BACs for painting of chromosomes 3 and 5 and in collaboration with Dr. M. Lysak and Dr. J. Fuchs developed multi-color CP technique for simultaneous visualization of all individual *Arabidopsis* chromosomes (published in the second paper). Analysis of chromosome rearrangements in T665-IST line by CP was performed by Young Min Kim (student from University of Kassel visiting IPK in March - April 2004) under my supervision (the results are unpublished). Experiments assessing chromosome rearrangement in EL702C line were performed by myself and are described in the third referred paper.

The part '**Interphase chromosomes: structural and functional organization**' is based on the paper Pecinka et al. (2004) *Chromosoma* *113*, 258-269. All experiments assessing association frequencies of homologous and heterologous CTs were performed by myself. Relative position of *FWA* gene to its CT was investigated by Dr. Veit Schubert in collaboration with myself (I have prepared painting probes and performed approximately half of FISH experiments). The frequency of somatic homologous pairing was analyzed by Dr. Veit Schubert (chromosome 1), Marco Klatté (chromosome 4) and myself (chromosome 3).

The part '**Influence of the repetitive transgenes and fluorescent chromatin tags on the interphase chromosome arrangement**' is based on the manuscript Pecinka et al., *J. Cell Sci.*, *submitted*. Initial experiments assessing the number of GFP spots in living nuclei of homozygous and hemizygous transgenic lines were performed by Dr. Naohiro Kato. All FISH experiments estimating pairing frequency of *lac* operator arrays and of flanking BACs F18C1 and MGL6 and their co-localization with heterochromatic chromocenters were performed by myself.

Eidesstattliche Erklärung

Hiermit erkläre ich, dass diese Arbeit von mir bisher weder der Mathematisch-Naturwissenschaftlich-Technischen Fakultät der Martin-Luther-Universität Halle-Wittenberg noch einer anderen wissenschaftlichen Einrichtung zum Zweck der Promotion eingereicht wurde.

Ich erkläre ferner, dass ich diese Arbeit selbständig und nur unter Zuhilfenahme der angegebenen Hilfsmittel und Literatur angefertigt habe.

Gatersleben, den

A. Pecinka

CURRICULUM VITAE

Name Ales Pecinka
Address Nova 9, Vresina, 747 20, Czech Republic
Birth 28. 01. 1978 in Opava, Czech Republic
Nationality Czech
Citizenship Czech Republic
Marital Status single

Education

1992 – 1996 Grammar school, Hlucin, Czech Republic
1996 – 2001 Palacky University in Olomouc, Czech Republic,
Faculty of Natural Sciences, Systematic Botany,
M.Sc. Thesis: “Taxonomy and distribution of the genus
Koeleria Pers. (*Poaceae*) in Czech Republic and Slovakia“
June 2001 Graduation as Master of Science, Mgr. (= M.Sc.)
Since September 2001 Ph.D. study at the Institute of Plant Genetics and Crop Plant
Research (IPK), Gatersleben, Germany

Appendix

Appendix: The tiling path of BAC clones used for chromosome painting of all five *Arabidopsis thaliana* chromosomes

Appendix: Table 1. The tiling path of BAC clones from **Arabidopsis chromosome 1** according to the MATDB (<http://mips.gsf.de/proj/thal/db/>). All BACs that were excluded from painting probes either because of a strong signal on Dot Blot and/or presence of mobile elements within annotated sequences in TIGR database are shown in grey.

part 1		part 2		part 3		part 4	
Clones	Genbank no.						
TEL1N	AC074298	T28K15	AC022522	F16L1	AC073942	F5D14	AC007767
T25K16	AC007323	F5O11	AC025416	T16E15	AC068562	T9G5	AC055769
F6F3	AC023628	T12C24	AC025417	F12K8	AC006551	F6N18	AC017118
F22L4	AC061957	F13K23	AC012187	T22J18	AC003979	F9L11	AC006424
T1N6	AC009273	F3F19	AC007357	F19G10	AF000657	T9L6	AC021045
F22M8	AC020622	T6J4	AC011810	T26J12	AC002311	T16O9	AC027035
T7I23	U89959	F13B4	AC027134	F26F24	AC005292	F10C21	AC051630
T6A9	AC064879	F21F23	AC027656	F28C11	AC007945	T1E4	AC069299
T14P4	AC022521	F16A14	AC068197	F5O8	AC005990	F14M2	AC010164
F22D16	AC009525	F7A19	AC007576	T23E23	AC002423	T3M13	AC022288
F10O3	AC006550	F14L17	AC012188	F3I6	AC002396	F12G12	AC015446
F15K9	AC005278	T5E21	AC010657	F21J9	AC000103	F23M19	AC007454
F21B7	AC002560	F10B6	AC006917	F5A9	AC004133	F7P12	AC023913
F21M11	AC003027	T15D22	AC012189	F4F7	AC079374	F12K21	AC023279
F20D22	AC002411	F9L1	AC007591	F2J7	AC079281	F21H2	AC007894
F19P19	AC000104	T16N11	AC013453	F14G11	AC084221	F11O6	AC018460
T1G11	AC002376	F7H2	AC034256	F28B23	AC079829	T32G9	AC079605
F13M7	AC004809	T24D18	AC010924	T1K7	AC013427	T9I1	AC069160
T7A14	AC005322	F3O9	AC006341	T24P13	AC006535	F12A4	AC023064
T25N20	AC005106	F19K19	AC011808	T2P11	AC005508	F15O4	AC007887
F3F20	AC007153	F17F16	AC026237	T7N9	AC000348	F14D7	AC021198
T20M3	AC009999	F6I1	AC051629	F17L21	AC004557	F10O5	AC027032
T21E18	AC024174	F20D23	AC007651	T17H3	AC005916	T22A15	AC021666
F9P14	AC025290	T13M22	AC026479	T22C5	AC012375	F5J5	AC006228
T2D23	AC068143	F28G4	AC007843	F28L5	AC079280	F15C21	AC025781
F12K11	AC007592	F1L3	AC022492	F13K9	AC069471	F16I10	AC079278
F4H5	AC011001	F11A6	AC034257	F3H9	AC021044	F7F23	AC021199
F10K1	AC067971	F2H15	AC034106	F3M18	AC010155	F28J9	AC007918
F22G5	AC022464	T10F20	AC034107	F1K23	AC007508	T15P17	AC025782
F24B9	AC007583	T10O22	AC069551	F28N24	AC021043	T32O22	AC079028
T6D22	AC026875	F15H18	AC013354	F15D2	AC068667	F1O3	AC068901
T23G18	AC011438	F25I16	AC026238	T3M22	AC079288	T32E20	AC020646
T27G7	AC006932	F6A14	AC011809	F1N18	AC008030	F28L22	AC007505
F22O13	AC003981	F14D16	AC068602	T1P2	AC022455	T18N24	AC074111
F7G19	AC000106	T29M8	AC069143	T2H7	AC074176	F8L2	AC087569
T12M4	AC003114	F18O14	AC025808	F12P21	AC073506	F2C1	AC074109
T31J12	AC006416	F14P1	AC024609	T4K22	AC025295	F12G6	AC007781
F14J9	AC003970	F6F9	AC007797	F26G16	AC009917	T28N5	AC067965
F21M12	AC000132	T20H2	AC022472	T5I8	AC007060	CEN1	
T27I1	AC004122	F14O10	AC026234	T17H7	AC004135	F25O15	AC074108
F14N23	AC005489	F5M15	AC027665	F17F8	AC000107	F9D18	AC007183
T10O24	AC007067	F2D10	AC069251	F28K20	AC004793	F9M8	AC083859
F20B24	AC009398	F9H16	AC007369	T19E23	AC007654	T4I21	AC022456
T16B5	AC007354	T22I11	AC012190	T8E3	AC027135	F5A13	AC008046
T19D16	U95973	F16F4	AC036104	F27M3	AC074360	F16M11	AC084241
T28P6	AC007259	F24J8	AC015447	F5M6	AC079041	F19C17	AC073433
T23J18	AC011661	F8K7	AC007727	T12O21	AC074309	F7F22	AC007534
F25C20	AC007296	T26F17	AC013482	F3C3	AC084165	T8D8	AC025815
F12F1	AC002131	F2E2	AC069252	F27G20	AC084110	F8D11	AC035249

Appendix: Table 1 (continued)

part 5		part 6		part 7		part 8	
Clones	Genbank no.						
F13A11	AC068324	F8L10	AC022520	F9N12	AC022355	F14O23	AC012654
F2H10	AC026757	F12M16	AC008007	F2K11	AC008047	F17M19	AC021665
F1121	AC005687	T3F20	AC018748	F24D7	AC011622	F28P5	AC069273
T10P12	AC007203	F22G10	AC024260	T12P18	AC010852	T9N14	AC067754
F2J6	AC009526	T18A20	AC009324	F22C12	AC007764	T10D10	AC016529
F28H19	AC006423	F15I1	AC006577	F15H21	AC066689	F28P22	AC010926
F9C16	AC022314	F20D21	AC005287	F1N19	AC009519	F3N23	AC008017
T7O23	AC074228	T22H22	AC005388	F13O11	AC006193	T18K17	AC010556
T18F15	AC084807	F14C21	AC069144	F16G16	AC009360	T9L24	AC012396
T12C22	AC020576	T7N22	AC073944	T23K8	AC007230	F6D5	AC079676
F27F5	AC007915	F7A10	AC027034	T8F5	AC004512	F25P22	AC012679
T2P3	AC084820	T18I3	AC079287	F5I14	AC001229	F2P9	AC016662
F2G19	AC083835	T5A14	AC005223	F1E22	AC007234	F9E11	AC079678
F8G22	AC079677	F20N2	AC002328	F12P19	AC009513	F1O17	AC020579
T3F24	AC015449	F14J16	AC002304	F15E12	AC026480	F1M20	AC011765
F16N3	AC007519	T6H22	AC009894	T6J19	AC066691	F25A4	AC008263
T2E6	AC012463	F14G9	AC069159	T27F4	AC020665	F9E10	AC013258
T6B12	AC079679	F13N6	AC058785	F28G11	AC074025	F22H5	AC025814
T2J15	AC051631	F25P12	AC009323	T12I7	AC079285	F1B16	AC023754
F21D18	AC023673	T8L23	AC079733	F4N21	AC013288	F1OA5	AC006434
F11A17	AC007932	F12K22	AC079732	T4O24	AC083891	T4O12	AC007396
T1N15	AC020889	F13D13	AC079991	F1O19	AC007152	T23E18	AC009978
F9P7	AC074308	T15M6	AC079604	F5A8	AC004146	F15M4	AC012394
F11I4	AC073555	T18I24	AC079131	F1N21	AC002130	F14G6	AC015450
T24P22	AC084242	F16M22	AC073943	T1F15	AC004393	F28O16	AC010718
F27K7	AC084414	F19C14	AC008051	F12B7	AC011020	F7O12	AC079283
F27J15	AC016041	F9K23	AC082643	F12A21	AC008113	F22K20	AC002291
F13F21	AC007504	F20B16	-	T23K23	AC012563	T14N5	AC004260
F14J22	AC011807	T4M14	AC027036	T22E19	AC016447	F2P24	AC078898
F10F5	AC079674	T30E16	AC009317	T2E12	AC015986	T5M16	AC010704
T18C15	AC074110	F23H11	AC007258	T26J14	AC011915	T32E8	AC012193
F2J10	AC015445	T2K10	AC005966	F24J5	AC008075	F28K19	AC009243
F14I3	AC007980	T13D8	AC004473	F14K14	AC011914	T11I11	AC012680
F11F12	AC012561	F8A5	AC002292	T6L1	AC011665	F3F9	AC013430
F17J6	AC079279	F23C21	AC079675	F4N2	AC008262	T30F21	AC007260
F4M15	AC079027	T7P1	AC018908	F23O10	AC018364	F9K20	AC005679
F8A12	AC079284	F11P17	AC002294	F10D13	AC073178	T8K14	AC007202
F23H24	AC079828	T1F9	AC004255	F24J1	AC021046	F20B17	AC010793
F11M15	AC006085	T25B24	AC005850	T6C23	AC013289	F19K16	AC011717
F5D21	AC024261	T13M11	AC005882	T17F3	AC010675	F18B13	AC009322
F19C24	AC025294	F8K4	AC004392	F20P5	AC002062	F5I6	AC018848
T14L22	AC015448	F19K23	AC000375	F17O7	AC003671	T21F11	AC018849
F5F19	AC006216	F24O1	AC003113	F24J13	AC010796	F23A5	AC011713
F9I5	AC022354	T3P18	AC005698	F5A18	AC011663	TEL1S	AC074299
F19K6	AC037424	F23N19	AC007190	F15H11	AC008148		
F6D8	AC008016	F16P17	AC011000	F23N20	AC016972		
F14G24	AC019018	F16M19	AC010795	F3I17	AC016162		

Appendix: Table 2. The tiling path of BAC clones from **Arabidopsis chromosome 2** according to the MATDB (<http://mips.gsf.de/proj/thal/db/>). All BACs that were excluded from painting probes either because of a strong signal on Dot Blot and/or presence of mobile elements within annotated sequences in TIGR database are shown in grey.

part 1		part 2		part 3		part 4	
Clones	Genbank no.						
F15B18	AC006837	T12J2	AC004483	F16F14	AC007047	F27C12	AL031369
F23H14	AC006200	CEN		F1P15	AC007195	T22F11	AC007070
F2I9	AC005560	T14C8	AC006219	T24I21	AC005825	F13B15	AC006300
T8O11	AC006069	F7B19	AC006586	F12A24	AC005167	F3N11	AC006053
T23K3	AC007069	T15D9	AC007120	F6P23	AC002354	F17H15	AC005395
F23I14	AC007265	F7K9	AC007311	T23A1	AC007127	T19L18	AC004747
F14H20	AC006532	F12P23	AC007264	F5J6	AC002329	T1D16	AC004484
F5O4	AC005936	T4D8	AC007188	MJB20	AC007584	T9J22	AC002505
T16F16	AC005312	T6A13	AC006250	T19E12	AC007509	F18A8	AC003105
T8K22	AC004136	T16I21	AC006570	T17A5	AF024504	F12C20	AC005168
T20F6	AC002521	F16G22	AC007261	T13L16	AC003952	T20P8	AC005623
T17M13	AC004138	F15K19	AC006429	T27K22	AC006201	F20F1	AC007154
T18E12	AC005313	T13H18	AC006136	F8D23	AC007212	T22O13	AC007290
T4M8	AC006284	F3K12	AC006419	T30D6	AC006439	F12K2	AC006233
F19B11	AC006836	F14P14	AC007166	F24H14	AC006135	F10A12	AC006232
T18C20	AC007196	T18O6	AC007672	MSF3	AC005724	F15K20	AC005824
F3C11	AC007167	F7E22	AC007187	F19F24	AC003673	T1E2	AC006929
F3L12	AC007178	F23M2	AC007045	T20K24	AC002392	F24D13	AC005851
T16B23	AC007293	T10J7	AC005897	F27F23	AC003058	T3B23	AC006202
T23015	AC007213	F24C20	AC007112	F3P11	AC005917	T1B3	AC006283
T1O3	AC006951	T27D6	AC007268	F6F22	AC005169	T17D12	AC006587
F7D11	AC007231	T4E5	AC007295	T2G17	AC006081	T8O81	AC007171
F28I8	AC006955	F10C8	AC007288	F11A3	AC006569	T11P11	AC007184
F1O13	AC007211	T18E17	AC007155	T13C7	AC007109	F8N16	AC005727
F15L11	AC007443	T19K21	AC006437	F23N11	AC007048	T9I4	AC005315
F5G3	AC007018	T17A11	AC006194	F5H14	AC006234	F16P2	AC004561
F16J10	AC007289	F15O11	AC006446	F26H11	AC006264	T27A16	AC005496
T20G20	AC006220	F14O4	AC007209	F7O24	AC007142	F6K5	AC007113
T3P4	AC007170	T26C18	AC007294	F3K23	AC006841	F23F1	AC004680
T25M19	AC007233	T10F5	AC007063	F2G1	AC007119	T27E13	AC004165
T17C22	AC006555	F13J11	AC006436	F7D8	AC007019	T9D9	AC002338
T6P5	AC005970	F17L24	AC006218	T16B14	AC007232	T6B20	U93215
F5K7	AC006413	F9B22	AC006528	T26C19	AC007168	T11J7	AC002340
F18P14	AC006918	T22C12	AC007197	F14M13	AC006592	F7F1	AC004669
F28N16	AC007235	F15N24	AC007210	T9I22	AC006340	T16B12	AC005311
T12H3	AC006420	T1O16	AC006304	T30L20	AC005617	F16D14	AC006593
T14A4	AC006161	T13P21	AC006067	T20K9	AC004786	T28P16	AC007169
T9F8	AC005561	T6B13	AC005398	F21P24	AC004401	T9H9	AC007071
T4E14	AC005171	F26C24	AC004705	T20D16	AC002391	F20M17	AC006533
T25N22	AC005693	T26I20	AC005396	F26B6	AC003040	F22D22	AC006223
T13E11	AC006217	T15J14	AC005957	F27L4	AC004482	T32F6	AC005700
F27C21	AC006527	F15A23	AC006298	T29E15	AC005170	T26B15	AC004681
F9A16	AC007662	F27O10	AC007267	F27D4	AC005967	F24L7	AC003974
T5M2	AC007730	F26H6	AC006920	T28I24	AC006403	T21L14	AC003033
T17H1	AC007143	F9O13	AC006248	F25P17	AC006954	F25I18	AC002334
T18C6	AC007729	F19G14	AC006438	F27A10	AC007266	F4P9	AC002332
T5E7	AC006225	F7H1	AC007134	F13D4	AC006585	T1B8	U78721

Appendix: Table 2 (continued)

part 5		part 6		part 7		part 8	
Clones	Genbank no.						
T14G11	AC002341	T8P21	AC007661	T3K9	AC004261	F16B22	AC003672
F13P17	AC004481	F16M14	AC003028	F13H10	AC005662	T13E15	AC002388
T31E10	AC004077	T19C21	AC004683	T26J13	AC004625	T14P1	AC007659
T29F13	AC003096	T6A23	AC005499	T32G6	AC002510	F4L23	AC002387
F19I3	AC004238	F13I13	AC007133	T11A7	AC002339	F17K2	AC003680
T4C15	AC004667	T7F6	AC005770	T6D20	U90439	F4I8	AC004665
T32F12	AC005314	T16B24	AC004697	T24P15	AC002561	T3F17	AC005397
T20F21	AC006068	F12L6	AC004218	MHK10	AC005956	F11C10	AC006526
F11F19	AC007017	F17A14	AC003674	F14N22	AC007087	F13A10	AC006418
F9C22	AC007135	T5I7	AC003000	F7D19	AC006931	T3A4	AC005819
F2H17	AC006921	T28M21	AF002109	F23E6	AC006580	F19D11	AC005310
F1O11	AC006919	F27I1	AC007658	MFL8	AC006224	F14M4	AC004411
F13K3	AC006282	T7M7	AF085279	F14B2	AC004450	T3D7	AC007236
T1J8	AC006922	T3G21	AC007020	T1O24	AC002335	T8I3	AC002337
T2N18	AC006260	T2P4	AC002336	F18O19	AC002333	T3B22	AC002535
F3G5	AC005896	T7D17	AC007660	F6E13	AC004005	F17A22	AC005309
F13M22	AC004684	T20B5	AC002409	F4I1	AC004521	T9J23	AC006072

Appendix: Table 3. The tiling path of BAC clones from **Arabidopsis chromosome 3** according to the MATDB (<http://mips.gsf.de/proj/thal/db/>). All BACs that were excluded from painting probes either because of a strong signal on Dot Blot and/or presence of mobile elements within annotated sequences in TIGR database are shown in grey. BACs labelled in blue were not provided by ABRC stock center and therefore were not tested on Dot Blot, however, these BACs did not contain repeats within annotated sequences in TIGR database.

part 1		part 2		part 3		part 4	
Clones	Genbank no.						
TEL3N	AC067753	F14P13	AC009400	MTO12	AB028620	MDB19	AB023036
T4P13	AC008261	F13M14	AC011560	MKP6	AB022219	MYM9	AP000377
T22N4	AC010676	T7M13	AC011708	MIG5	AB026646	F14O13	AP001297
T13O15	AC010870	F9F8	AC009991	MEB5	AB019230	MUJ8	AB028621
F4P13	AC009325	F11B9	AC073395	MBG14	AB026641	K13K6	AP002037
F28J7	AC010797	F24K9	AC008153	MRC8	AB020749	K7M2	AP000382
F1C9	AC011664	T19F11	AC009918	MIE15	AP000414	MXP5	AP002048
F14P3	AC009755	F26K24	AC016795	MYF24	AB026658	MOB24	AB020746
F11A12	AC068900	T21B14	AC069473	K24M9	AP001303	MSD24	AP000740
F16B3	AC021640	F28J15	AC069472	MVE11	AB026654	K7P8	AB028609
F13E7	AC018363	T2E22	AC069474	MCB22	AP002039	K3G3	AP000412
T17B22	AC012328	MBK21	AB024033	K13E13	AP000735	MJL12	AB026647
T21P5	AC009895	MJM20	AC023838	MHP21	AP002041	MTE24	AP000376
T12J13	AC009327	MGH6	AC024128	MV111	AP000419	MWL2	AB025639
F20H23	AC009540	MJG19	AP000375	MLD14	AB025624	T5M7	AP001313
T11I18	AC011698	MJH23	AP002042	T31J18	AP002065	K13N2	AB028607
T6K12	AC016829	MDC11	AB024034	MMB12	AP000417	K9I22	AP000599
T27C4	AC022287	MRP15	AP000603	MPN9	AB025631	MPE11	AB023041
F7O18	AC011437	K20M4	AP002038	MZE19	AP002050	MJL14	AP000601
T9J14	AC009465	MMM17	AP001307	MAL21	AP000383	MTC11	AB024038
T12H1	AC009177	MCP4	AB028610	MQC12	AB024036	F20C19	AP001298
F22F7	AC009606	MDC16	AB019229	K10D20	AP000410	MFE16	AB028611
F18C1	AC011620	MAG2	AP000600	F3H11	AP002034	MLJ15	AB026648
F10A16	AC012393	MLE3	AP000416	MOE17	AB025629	MDJ14	AB016889
F2O10	AC013454	MLN21	AB022220	MFD22	AP001304	MQP17	AP000602
F24F17	AC068073	MOA2	AB028617	MSA6	AP000604	MOJ10	AB026649
F28L1	AC018907	MIE1	AB023038	MXL8	AB023045	MYF5	AP001312
F24P17	AC011623	T21E2	AP002061	MHC9	AP001305	K17E12	AP000381
F5E6	AC020580	K15M2	AP000370	MIL23	AB019232	K1G2	AB024028
T8E24	AC036106	F4B12	AP001299	MSD21	AB025634	MMJ24	AB025626
F3E22	AC023912	K7L4	AC023839	MEK6	AP000739	MGF10	AB018114
F17A9	AC016827	MJK13	AC024081	MZN24	AB028622	K16N12	AP000371
T1B9	AC012395	MQD17	AB028619	MKA23	AP001306	K24A2	AP001302
F21O3	AC009853	MSJ11	AB017071	MMP21	AP002046	MMG15	AB028616
MLP3	AC009176	MVC8	AB026653	MCB17	AB022215	MIG10	AP000415
F17A17	AC013483	MSL1	AB012247	F16J14	AP000731	T19D11	AP002056
T8G24	AC074395	MYA6	AB023046	MW123	AB022223	MZF16	AP002051
F17O14	AC012562	MDC8	AP000373	F5N5	AP001300	MFJ20	AB026644
T16O11	AC010871	MGL6	AB022217	MXC7	AB026655	T20D4	AP002059
MZB10	AC009326	K20I9	AB028608	K13C10	AP000734	MZN14	AP000420
F3L24	AC011436	MUH15	AP001308	K14B15	AB025608	T19N8	AP002057
F11F8	AC016661	K14A17	AB026636	F28F4	AP000733	MLD15	AP000386
F8A24	AC015985	MCE21	AP000384	MLM24	AB015474	MYI13	AP002049
T22K18	AC010927	MGD8	AB022216	MEE5	AP000374	K5K13	AB025615

Appendix: Table 3 (continued)

part 5		part 6		part 7		part 8	
Clones	Genbank no.						
MRI12	AP000388	T15D2	AP002054	F9K21	AL138657	T5N23	AL138650
MXE2	AB018121	CEN		T6D9	AL157735	F28P10	AL049655
MUO22	AP001310	T25F15	AC009529	F16L2	AL162459	T15C9	AL132970
MXO21	AB026657	F23H6	AC011621	F12M12	AL355775	T26I12	AL132954
MMF24	AP002045	T28G19	AC009328	F18L15	AL133298	T22E16	AL132975
MUO10	AP001309	5SrDNA		F12A12	AL133314	F1I16	AL161667
T13B17	AP002459	F21A14	AC016828	T6H20	AL096859	F27K19	AL163832
MWE13	AP002457	T4P3	AC009992	F13I12	AL133292	F18O21	AL163763
MTO24	AP000606	T14A11	AC012327	T21L8	AL096860	T5P19	AL163972
T13J10	AP002052	T26P13	AC009261	F1P2	AL132955	T8M16	AL390921
MOD1	AB028618	T18B3	AC011624	T23J7	AL049746	F24I3	AL138655
T26G12	AP002064	5SrDNA		T17F15	AL049658	F28O9	AL137080
K17E7	AP000736	F4M19	AL356013	T24C20	AL096856	T8H10	AL133248
T20F20	AP002060	T27B3	AL137079	T29H11	AL049659	F15B8	AL049660
MIL15	AB028615	F26B15	AL138645	T8P19	AL133315	T10K17	AL132977
T6J22	AP001314	T14K23	AL132909	T21J18	AL132963	F9D24	AL137081
MVA11	AP001311	T32A11	AL138653	T2J13	AL132967	F14P22	AL137082
MSJ3	AP000389	T12K4	AL138640	F2K15	AL132956	T20N10	AL353032
MQP15	AB016878	F7P3	AL138663	T9C5	AL132964	F17J16	AL163527
MED16	AP000738	T21C14	AL138639	T16K5	AL132965	F25L23	AL356014
MED5	AB026642	F18P9	AL138654	F3A4	AL132978	T16L24	AL138659
F21A17	AP000732	F7M19	AL138643	F11C1	AL132976	F24G16	AL138647
T4A2	AP002066	T6L19	AL391731	T20E23	AL133363	T2O9	AL138658
MIF6	AB028614	F7K15	AL353871	T3A5	AL132979	F27H5	AL163852
F11I2	AP001296	T5C2	AL138664	F18B3	AL049862	T8B10	AL138646
K11J14	AP000411	T18D12	AL138644	F24M12	AL132980	T4C21	AL162295
MJ16	AP002043	F22J12	AL391734	F26O13	AL133452	T27I15	AL358732
T22P15	AP002461	F23N14	AL138638	T18N14	AL132968	T20K12	AL137898
T22B15	AP002062	T28A8	AL162691	AtEM1	AF049236	F2A19	AL132962
T22C2	AP002458	T15B3	AL163975	F4F15	AL049711	F15G16	AL132959
T10I3	AP002058	F26G5	AL353814	T25B15	AL132972	F21F14	AL138642
F8N14	AP001301	T10D17	AL353865	F22O6	AL050300	T17J13	AL138651
T8O3	AP002068	T22K7	AL138641	F3C22	AL353912	T12C14	AL162507
F1M23	AP002033	F14L2	AL353818	F8J2	AL132969	F26K9	AL162651
F9K1	AP002036	T18B22	AL138652	T4D2	AL132958	T20O10	AL163816
F6H5	AP002035	T32N15	AC002534	F4P12	AL132966	F16M2	AL138648
T8N9	AP002462	F28D10	AL391254	F5K20	AL132960	MAA21	AL163818
F1D9	AP002460	F14D17	AL353992	F24B22	AL132957		
T7B9	AP002067	T14D3	AL138649	T12E18	AL132971		
T13O13	AP002053	F18N11	AL132953	T14E10	AL138656		

Appendix: Table 4. The tiling path of BAC clones from **Arabidopsis chromosome 4** according to the MATDB (<http://mips.gsf.de/proj/thal/db/>). Clones used for chromosome painting (according to Lysak et al., Plant J 28:689-697, 2001) are unlabeled. All BACs that were either excluded from painting probes or not provided by ABRC stock center are shown in grey..

part 1		part 2		part 3		part 4	
Clones	Genbank no.						
T15P10	AF167571	F9M13	AC006267	T18B16	AL021687	T16L4	AL079344
F6N15	AF069299	T12G13	AL080252	T5K18	AL022580	F27B13	AL050352
F5I10	AF013293	T28D5	AL109819	F24J7	AL021768	F6G3	AL078464
F6N23	AF058919	C18G5	AL110116	T16H5	AL024486	F9N11	AL109796
F15P23	AF128392	T15F16	AF076275	F18F4	AL021637	F17I23	AF160182
T18A10	AF013294	T3F12	AC002983	F1C12	AL022224	T10C21	AL109787
F3I3	AL080237	T32A17	AL161813	F9F13	AL080253	F6I18	AL022198
F2N1	AF007269	T3H13	AF128396	F21C20	AL080254	F6E21	AL049914
F3D13	AF069300	F23J3	AC005359	T13K14	AL080282	F8F16	AL021633
F11O4	AF096370	T8A17	AF072897	F7J7	AL021960	F3L17	AL080283
T15B16	AF104919	T30A10	AL117386	T6K22	AL031187	F28M20	AL031004
T7B11	AC007138	T15G18	AC006567	F18E5	AL022603	F11C18	AL049607
T10M13	AF001308	T25P22	AL161831	F17L22	AL035527	F10N7	AL021636
T2H3	AF075597	F17A8	AL049482	T8O5	AL021890	F10M6	AL021811
T14P8	AF069298	T5L19	AL049481	F1N20	AL022140	F8B4	AL034567
T10P11	AC002330	F28M11	AL049487	T10I14	AL021712	L23H3	AL050398
T5J8	AC004044	F24G24	AL049488	F7K2	AL033545	F4D11	AL022537
T4I9	AF069442	F7L13	AL049524	T12H17	AL021635	T16I18	AL049915
F4C21	AC005275	T4F9	AL049523	F7H19	AL031018	F26P21	AL031804
F9H3	AF071527	T12H20	AF080119	F21P8	AL022347	F4I10	AL035525
T5L23	AC005142	F25I24	AL049525	F16G20	AL031326	F17M5	AL035678
T5H22	AF096372	T22B4	AL049876	F9D16	AL035394	T16L1	AL031394
T7M24	AF077408	F8L21	AL096882	T32A16	AL078468	F17I5	AL031032
T25H8	AF128394	F25E4	AL050399	T19F6	AL109619	F28A23	AL021961
T24M8	AF077409	T5C23	AL049500	T22A6	AL078637	F10M10	AL035521
T24H24	AF075598	T26M18	AL078606	F22K18	AL035356	T4L20	AL023094
T27D20	AF076274	F16J13	AL049638	F6I7	AL049657	F11I11	AL079347
T19B17	AF069441	T4C9	AL080318	F13M23	AL035523	M4E13	AL022023
T26N6	AF076243	T1P17	AL049730	F24A6	AL035396	T12J5	AL035522
F4H6	AF074021	T20K18	AL049640	T30C3	AL079350	F23E12	AL022604
T19J18	AF149414	F25G13	AL079349	M7J2	AL022197	F15J1	AL117188
T4B21	AF118223	F17N18	AL049751	L73G19	AL050400	F8D20	AL031135
T1J1	AF128393	T9E8	AL049608	F14M19	AL049480	F4B14	AL031986
T32N4	AF162444	T6G15	AL049656	F20B18	AL049483	T19K4	AL022373
C17L7	AC012392	F18A5	AL035528	T25K17	AL049171	F23E13	AL022141
C6L9	AC012477	ATFCA0	Z97335	M3E9	AL022223	ATAP22	Z99708
T1J24	AF147263	ATFCA1	Z97336	T15N24	AL078465	ATAP21	Z99707
F6H8	AF178045	ATFCA2	Z97337	F10M23	AL035440	F6G17	AL035601
F2I12	AF147261	ATFCA3	Z97338	T24A18	AL035680	F19F18	AL035605
CEN		ATFCA4	Z97339	M4I22	AL030978	T28I19	AL035709
F14G16	AF147260	ATFCA5	Z97340	F27G19	AL078467	F20D10	AL035538
F28D6	AF147262	ATFCA6	Z97341	T29A15	AL035602	F22I13	AL035539
T3E15	AF147264	ATFCA7	Z97342	T27E11	AL049770	F20M13	AL035540
T14A16	AF160181	ATFCA8	Z97343	T13J8	AL035524	T9A14	AL035656
F10A2	AF147259	ATFCA9	Z97344	F26K10	AL049803	F19H22	AL035679
T6L9	AF147265	T6K21	AL021889	F20O9	AL021749	T22F8	AL050351
F5K24	AF128395	F15J5	AL110123	T5F17	AL049917	F23K16	AL078620
T24G23	AC006268	T9A21	AL021713	F16A16	AL035353	T19P19	AL022605
F1K3	AC006266	F28J12	AL021710	F25O24	AL078469	T5J17	AL035708
T17A2	AF160183	F28A21	AL035526	F19B15	AL078470		
T13D4	AC007125	F13C5	AL021711	F17A13	AL096692		

Appendix: Table 5. The tiling path of BAC clones from **Arabidopsis chromosome 5** according to the MATDB (<http://mips.gsf.de/proj/thal/db/>). All BACs that were excluded from painting probes either because of a strong signal on Dot Blot and/or presence of mobile elements within annotated sequences in TIGR database are shown in grey.

part 1		part 2		part 3		part 4	
Clones	Genbank no.						
F7J8	AL137189	T22P22	AL163814	MWD9	AB007651	F3F24	AC018632
T10O8	AL161746	F14F18	AL163812	MQJ16	AB012244	F23C8	AC018928
F7A7	AL161946	MXC9	AB007727	MDJ22	AB006699	T3P1	AC069329
T20L15	AL162351	T2L20	AL592312	K5A21	AB024030	F7I20	AC069555
T7H20	AL162508	T24H18	AL353013	K8E10	AB025618	F17M7	AC069552
T1E22	AL162874	T19L5	AL391711	MRN17	AB005243	F19I11	AC069554
T22P11	AL162971	T31B5	AL163491	T20O7	AB026660	T21M13	-
F9G14	AL162973	T22N19	AL163572	MYJ24	AB006708	CEN	
F15A17	AL163002	T6I14	AL391710	MKD15	AB007648	F13C19	AF296827
F12E4	AL162751	MSH12	AB006704	T32G24	AB025642	F14C23	AF296828
F17C15	AL162506	MXE10	AB011484	K19M13	AB018110	F18O9	AF296831
MED24	AB005235	MAC12	AB005230	MQM1	AB025633	T15F17	AF262042
F8F6	AL162873	MUA22	AB007650	MRO11	AB005244	F3D18	AF296829
F21E1	AL391716	F18O22	AL163817	MZF18	AB009056	F15I15	AF296826
T19N18	-	T15N1	AL163792	MLE8	AB010696	T6F8	AC063973
T32M21	AL162875	T9L3	AL391149	K12G2	AB016883	T29A4	AC069557
T1E3	AL162972	F2G14	AL391146	MOP9	AB006701	F19N2	AC051625
MUK11	AB008271	F8M21	AL353993	K16H17	AB016884	F18A12	AC069553
MLG18	AB025625	T20K14	AL391143	T31K7	AB025641	T32B3	AC024226
MUG13	AB005245	F14F8	AL391144	K18P6	AB010068	T3J11	AC019012
K2A11	AB018111	F1N13	AL391145	MXC17	AB016881	F11P10	AC018660
K18I23	AB010692	T21H19	AL391148	T4C12	AL392145	T5E15	AC019013
MOP10	AB005241	MQK4	AB005242	F6A4	AF069716	T2L5	AF096371
MJJ3	AB005237	MTG13	AB008270	T11H3	AC005964	T9E19	AF104920
K18J17	AB017060	F5E19	AL391147	F21J6	AC006259	F7N22	AF058825
K16F4	AP002030	F2K13	AL391141	F18G18	AC006258	T25C13	AF080121
MBL20	AP002544	MKP11	AB005238	T14C9	AC006601	T26D22	AF058826
MHF15	AB006700	T10B6	AL391142	T5I5	AC084432	K21B8	AB025611
F15M7	AP002543	K3M16	AL391150	F18A17	AC005405	MOK9	AB015477
MPH15	AP002032	K10A8	AL391151	T1N24	AF149413	K2K18	AB023031
MOJ9	AB010697	MVA3	AB006706	T19G15	AC005965	MJE4	AB013393
T28J14	AL163652	MPI7	AB011480	F9D12	AF077407	MXH1	AB011485
T2I1	AL163912	MCM23	AB015473	F21E10	AF058914	MWP19	AB020753
MBK20	AB010070	MRG7	AB012246	F2P16	AF007270	MIK22	AB005236
MXM12	AB005249	F20L16	AC051626	F15P11	AF160760	F14A1	AB025602
F13G24	AL133421	T28N17	AC069328	T21B4	AF007271	MEE13	AB026643
T22D6	AL357612	T1A4	AC051627	F21A20	AC007123	MAB16	AB018112
F8L15	AL392174	F17K4	AC068655	F15A18	AC007478	T30G6	AB026661
MAH20	AB006697	T16G12	AC068809	T1G16	AC069556	CIC5B3	AP002549
T2K12	AL590346	T24G5	AC069326	F14I23	AC007399	F24C7	AP002029
T5E8	AL391712	F7K24	AF296837	F15F15	AC007627	MPK17	AP000418
F17I14	AL353994	T20D1	AF296830	T24G3	AC006192	F5H8	AB025605
MYH9	AB016893	T29J13	AF296838	F26C17	AF177535	MLF18	AB016877
T31P16	AL356332	F28I16	AF296836	T8M17	AF296835	K15O15	AB024026
F18D22	AL360334	F5O24	AF296825	F21B23	AF262038	MJG14	AB017068
F12B17	AL353995	F7C8	AF296833	F24J2	AF262039	MSK20	AP000605
MAJ23	AL392144	T1M15	AF296832	T26D3	AF262043	MNJ8	AB017069
T30N20	AL365234	F22D1	AF296834	T10I18	AF262040	T25O11	AP000607
T5K6	AL391222	T10F18	AC069325	F4I4	AF272705	MPA22	AB025630
F2I11	AL360314	F13M11	-	T32B20	AF262041	K12B20	AB018107
F15N18	AL163815	T6G21	AL589883	F7P1	AF272706	T31G3	AB026662

Appendix: Table 5 (continued)

part 5		part 6		part 7		part 8	
Clones	Genbank no.						
K22F20	AB016873	K23L20	AB016874	F17P19	AB025603	MGO3	AB019231
K18L3	AB012241	K21C13	AB010693	K24M7	AB019226	F15L12	AB026632
K19A23	AB025610	K17O22	AB019224	T4M5	AP000378	K9B18	AB015471
F16F17	AB028606	K18C1	AB012240	F6N7	AB025606	MUF9	AB011483
MXA21	AB005247	K9E15	AB020744	MXC20	AB009055	MUP24	AB005246
MSI17	AB011481	MFC19	AB018113	MNB8	AB018116	MAE1	AB015472
MXI10	AB005248	K2N11	AB022213	MFH8	AB025622	MSL3	AB008269
MBB18	AB005231	MRA19	AB012245	K19E1	AB013388	MAF19	AB006696
MKD10	AB011478	K15I22	AB016870	MYN8	AB020754	MFB13	AB010073
K15E6	AB009048	MCL19	AB006698	MNC6	AB015476	MCI2	AB016887
MXF12	AB016892	MDE13	AB025620	MGN6	AB017066	K11J9	AB012239
K3K3	AB010694	MPL12	AB010698	K6O8	AB025616	MAC9	AB010069
MUL8	AB009054	K11I1	AB019223	K19P17	AB007644	K22G18	AB022212
MIJ24	AB012243	F10E10	AB028605	MJP23	AB018115	MTG10	AB016880
MKM21	AB016876	MZA15	AB016882	K18G13	AB013387	MMI9	AB019235
K13H13	AB024023	MSD23	AB022221	MDK4	AB010695	K19B1	AB015469
MYH19	AB010077	MQD22	AB013394	GA469	AP000380	MRG21	AB020751
MUD12	AB022222	K14A3	AB025609	F24B18	AB026634	MQB2	AB009053
MSN9	AB010699	MQL5	AB018117	MRB17	AB016879	MJH22	AB009051
MPO12	AB006702	MNJ7	AB025628	K5F14	AB022214	MDC12	AB008265
K21I16	AB017062	MGC1	AB028612	MBG8	AB005232	K9H21	AB023035
MNF13	AB009052	MCA23	AB016886	K13P22	AB017059	MLE2	AB007649
K1B16	AB015470	K16F13	AB024025	MCO15	AB010071	MBK5	AB005234
MHK7	AB011477	MDN11	AB017064	MTE17	AB015479	MGI19	AB007646
MMG1	AB023040	MIF21	AB023039	MWC10	AB023043	MBM17	AB019227
MEE6	AB010072	K23F3	AP000372	MDF20	AB009050	MHJ24	AB008266
K1O13	AB019225	MJE7	AB020745	MWJ3	AB018120	MSJ1	AB008268
MYC6	AB006707	K15N18	AB015468	MYN21	AB026659	T12B11	AB025640
MPK23	AB020748	K24G6	AB012242	MDA7	AB011476	MUB3	AB010076
MBK23	AB005233	K19E20	AB017061	K24C1	AB023029	MVP7	AB025637
MUF8	AB025635	K20J1	AB023028	MXK23	AB026656	MXK3	AB019236
K16L22	AB016871	K21P3	AB016872	MCD7	AB009049	F15O5	AB026633
MJC20	AB017067	K7J8	AB023034	MKN22	AB019234	MQN23	AB013395
K5J14	AB023032	K6M13	AB023033	MIK19	AB013392	MNA5	AB011479
MDH9	AB016888	MNI5	AB025627	MPI10	AB020747	K19O4	AB026638
K16E1	AB022210	K2I5	AB025613	MHM17	AB024035	K21L13	AB026639
MFO20	AB013391	K21G20	AB025612	MUL3	AB023042	MPA24	AB010075
MJB21	AB007647	K9P8	AB024032	MJB24	AB019233	K22J17	AB020743
MBD2	AB008264	MPP21	AB026650	MSF19	AB016891	K14B20	AB018108
MRD20	AB020750	K6A12	AB024031	MUA2	AB011482	K2A18	AB011474
MMG4	AB008267	MXI22	AB012248	MRI1	AB018118	K1L20	AB022211
K24F5	AB023030	MBA10	AB025619	MTI20	AB013396	K1F13	AB013389
MNL12	AB017070	MFB16	AB023037	F2C19	AB026635	MSN2	AB018119
MWF20	AB025638	K7B16	AB025617	K21L19	AB024029	MUD21	AB010700
K9D7	AB016875	K16E14	AB026637	MCK7	AB019228	K8A10	AB026640
MQO24	AB026652	K3K7	AB017063	MQJ2	AB025632	K21H1	AB020742
MQD19	AB026651	MWD22	AB023044	MZN1	AB020755	K3G17	AB025614
F6B6	AP000368	MFG13	AB025621	K19M22	AB016885	K8K14	AB007645
MRH10	AB006703	K17N15	AB018109	K18B18	AB024027	K9I9	AB013390
MLN1	AB005239	K10D11	AB025607	MNC17	AB016890	LA522	AP000737
K9L2	AB011475	MIO24	AB010074	F2O15	AB025604		
MFC16	AB017065	MJM18	AB025623	MTH12	AB006705		
K15C23	AB024024	MSG15	AB015478	MMN10	AB015475		

Appendix: Table 6 Dimensions and volumes of different types of nuclei used for computer model simulations. (Per organ and ploidy level the mean values were used.)

Organ	Ploidy	Nuclear shape	<i>n</i>	Axis length (μm)			Volume (μm^3)
				x	y	z	
root	2C	sphere	30	5.2	4.1	1.9	22.4
		spindle	30	9.4	3.2	1.9	30.0
		rod	31	14.3	1.8	1.8	25.4
	4C	sphere	32	6.6	5.3	2.2	43.5
		spindle	31	10.2	3.6	2.2	43.8
		rod	31	18.8	2.4	2.1	47.5
leaf	2C	sphere	32	5.1	4.4	2.1	25.7
		spindle	32	7.1	3.7	2.0	27.9
		rod	32	10.3	2.5	2.0	26.4
	4C	sphere	32	6.1	5.2	2.0	34.4
		spindle	32	8.7	4.4	2.2	43.4
		rod	32	12.7	3.0	2.1	41.3

Appendix: Table 7 Experimentally observed association of all homologous and heterologous CT combinations in 4C spheric and spindle shaped 4C leaf nuclei

Chromosome combination	Experimentally observed associations					
	spheric nuclei (<i>n</i> =29; 56.9%)		spindle nuclei (<i>n</i> =22; 43.1%)		Σ (<i>n</i> =51)	
	<i>n</i>	%	<i>n</i>	%	<i>n</i>	%
1-1	26	89.7	19	86.4	45	88.2
1-2	27	93.1	22	100.0	49	96.0
1-3	29	100.0	22	100.0	51	100.0
1-4	29	100.0	21	95.5	50	98.0
1-5	29	100.0	22	100.0	51	100.0
2-2	24	82.8	15	68.2	39	76.4
2-3	27	93.1	22	100.0	49	96.0
2-4	29	100.0	20	90.9	49	96.0
2-5	28	93.1	22	100.0	50	98.0
3-3	24	82.8	17	77.3	41	80.3
3-4	29	100.0	20	90.9	49	96.0
3-5	28	93.1	22	100.0	50	98.0
4-4	24	82.8	16	72.7	40	78.4
4-5	29	100.0	20	90.9	49	96.0
5-5	24	82.8	21	95.5	45	88.2

Appendix: Table 8 Values predicted by the SCD model for random association frequency of all homologous and heterologous CT combinations in nuclei of the three predominant nuclear shapes

Chromosome combination	SCD model prediction					
	spheric nuclei ($n=10^3$)		spindle nuclei ($n=10^3$)		rod-shaped nuclei ($n=10^3$)	
	<i>n</i>	%	<i>n</i>	%	<i>n</i>	%
1-1	934	93.4	747	74.7	445	44.5
1-2	1000	100.0	980	98.0	896	89.6
1-3	1000	100.0	986	98.6	904	90.4
1-4	1000	100.0	972	97.2	901	90.1
1-5	1000	100.0	985	98.5	921	92.1
2-2	817	81.7	657	65.7	436	43.6
2-3	999	99.9	969	96.9	881	88.1
2-4	995	99.5	967	96.7	865	86.5
2-5	1000	100.0	973	97.3	899	89.9
3-3	852	85.2	674	67.4	436	43.6
3-4	997	99.7	968	96.8	884	88.4
3-5	1000	100.0	965	96.5	900	90.0
4-4	785	78.5	560	56.0	381	38.1
4-5	1000	100.0	942	94.2	870	87.0
5-5	905	90.5	635	63.5	419	41.9

Appendix: Table 9 Experimentally observed associations of chromosome-arm territories in root and leaf nuclei of different shape and DNA content; T=top arm, B=bottom arm, +=associated, -=separated

Homologues	Nuclei					Experimentally observed associations							
	Organ	Ploidy	Shape	<i>n</i>	%	T+B+		T+B-		T-B+		T-B-	
						<i>n</i>	%	<i>n</i>	%	<i>n</i>	%	<i>n</i>	%
Chromosome 1	leaf	2C	sphere	85	70.2	46	54.1	21	24.7	4	12.9	7	8.3
			spindle	29	24.0	9	31.1	3	10.3	7	24.1	14	34.5
			rod	7	5.8	2	28.6	0	0.0	0	0.0	5	71.4
			Σ	121	100.0	57	47.1	24	19.8	18	14.9	22	18.2
		4C	sphere	34	34	14	41.2	7	20.6	5	14.7	8	23.5
			spindle	51	51	25	49.0	11	21.6	7	13.7	8	15.7
			rod	15	15	8	53.4	2	13.3	0	0.0	5	33.3
			Σ	100	100.0	47	47.0	20	20.0	12	12.0	21	21.0
		8C	sphere	33	32.7	16	48.5	3	9.1	5	15.1	9	27.3
			spindle	62	61.4	27	43.6	12	19.3	7	11.3	16	25.8
			rod	6	5.9	0	0.0	2	33.3	2	33.3	2	33.3
			Σ	101	100.0	43	42.6	17	16.8	14	13.8	27	26.8
	root	2C	sphere	15	12.5	8	53.3	4	26.7	2	13.3	1	6.7
			spindle	53	44.2	24	45.3	4	7.5	9	17.0	16	30.2
			rod	52	43.3	13	25.0	11	21.1	5	9.6	23	44.2
			Σ	120	100.0	45	37.5	19	15.8	16	13.4	40	33.3
		4C	sphere	15	12.5	5	33.3	4	26.7	5	33.3	1	6.7
			spindle	71	59.2	30	42.3	17	23.9	17	23.9	7	9.9
			rod	34	28.3	7	20.6	14	41.2	7	20.9	6	17.6
			Σ	120	100.0	42	35.0	35	29.2	29	24.2	14	11.6
		8C	sphere	13	10.8	9	69.2	1	7.7	1	7.7	2	15.4
			spindle	98	81.7	44	44.9	16	16.3	16	16.3	22	22.4
			rod	9	7.5	2	22.2	1	11.1	0	0.0	6	66.7
			Σ	120	100.0	55	45.8	18	15.0	17	14.2	30	25.0
Chromosome 2	leaf	2C	sphere	62	51.6	33	53.2	5	8.1	7	11.3	17	27.4
			spindle	50	41.7	21	42.0	3	6.0	14	28.0	12	24.0
			rod	8	6.7	1	12.5	0	0.0	2	25.0	5	62.5
		Σ	120	100.0	55	45.8	8	6.7	23	19.2	34	28.3	
		4C	sphere	54	45.0	23	42.6	3	5.6	15	27.8	13	24.1
			spindle	61	50.8	29	47.5	4	6.6	9	14.7	19	31.1
	rod		5	4.1	2	40.0	0	0.0	3	60.0	0	0.0	
	Σ	120	100.0	54	45.0	7	5.8	27	22.5	32	26.7		
	leaf	4C	sphere	51	50	25	49.0	14	27.4	3	5.9	9	17.6
			spindle	50	49	22	43.1	13	25.5	3	5.9	11	21.6
			rod	1	1	0	0.0	0	0.0	1	100.0	0	0.0
	Σ	102	100.0	48	47.0	27	26.5	7	6.9	20	19.6		
Chromosome 4	leaf	2C	sphere	49	40.8	23	47.0	2	4.0	11	22.5	13	26.5
			spindle	53	44.2	23	43.4	2	3.8	14	26.4	14	26.4
			rod	18	15.0	5	27.8	0	0.0	6	33.3	7	38.9
		Σ	120	100.0	51	42.5	4	3.3	31	25.8	34	28.4	
		4C	sphere	76	63.3	32	41.6	7	9.0	19	24.7	19	24.7
			spindle	41	34.2	14	35.0	5	12.5	12	30.0	9	22.5
	rod		3	2.5	1	33.3	0	0.0	1	33.3	1	33.3	
	Σ	120	100.0	47	39.2	12	10.0	32	26.7	29	24.1		
	leaf	8C	sphere	37	33.0	19	51.4	8	21.6	4	10.8	6	16.2
			spindle	68	60.7	27	39.6	15	22.1	8	11.8	18	26.5
			rod	7	6.3	1	14.3	1	14.3	0	0	5	71.4

			Σ	111	100.0	47	42.0	24	21.4	12	10.7	29	25.9
	root	2C	sphere	13	10.8	7	53.8	2	15.4	2	15.4	2	15.4
			spindle	76	63.4	28	36.8	5	6.6	24	31.6	19	25.0
			rod	31	25.8	10	32.3	4	12.9	5	16.1	12	38.7
			Σ	120	100.0	47	39.2	10	8.3	28	23.3	35	29.2
		4C	sphere	23	18.8	8	34.8	1	4.3	7	30.4	7	30.4
			spindle	71	58.2	36	50.7	4	5.6	13	18.3	18	25.4
			rod	28	23.0	9	32.2	3	10.7	4	14.3	12	42.8
			Σ	122	100.0	53	43.4	8	6.6	24	19.7	37	30.3
		8C	sphere	37	28.5	20	54.1	11	29.1	3	8.1	3	8.1
			spindle	82	63.0	34	41.5	20	24.4	10	12.2	18	21.9
			rod	11	8.5	5	45.4	2	18.2	1	9.1	3	27.3
			Σ	130	100.0	59	45.4	33	25.3	14	10.8	24	18.5
Chromosome 5	leaf	4C	sphere	59	51.3	28	47.4	7	11.9	12	20.3	9	15.2
			spindle	55	47.8	29	52.7	6	10.9	10	18.2	13	23.6
			rod	1	0.9	0	0.0	0	0.0	1	100.0	0	0.0
			Σ	115	100.0	57	49.6	13	11.3	23	20.0	22	19.1

Appendix: Table 10 Values predicted by the SCD model for random association frequency of homologous chromosome-arm territories in nuclei of the three predominant nuclear shapes; T=top arm, B=bottom arm, +=associated, -=separated

Homologues	Nuclear shape	n	SCD model prediction							
			T+B+		T+B-		T-B+		T-B-	
			n	%	n	%	n	%	n	%
Chromosome 1	spheric	10^3	599	59.9	131	13.1	149	14.9	121	12.1
	spindle	10^3	482	48.2	108	10.8	116	11.6	294	29.4
	rod	10^3	236	23.6	91	9.1	103	10.3	570	57.0
Chromosome 2	spheric	10^3	391	39.1	33	3.3	436	43.6	212	21.2
	spindle	10^3	263	26.3	18	1.8	332	33.2	387	38.7
	rod	10^3	187	18.7	18	1.8	211	21.1	584	58.4
Chromosome 3	spheric	10^3	489	48.9	258	25.8	86	8.6	167	16.7
	spindle	10^3	387	38.7	148	14.8	48	4.8	417	41.7
	rod	10^3	235	23.5	110	11.0	55	5.5	600	60.0
Chromosome 4	spheric	10^3	252	25.2	17	1.7	473	47.3	258	25.8
	spindle	10^3	199	19.9	9	0.9	304	30.4	488	48.8
	rod	10^3	148	14.8	9	0.9	190	19.0	653	65.3
Chromosome 5	spheric	10^3	570	57.0	191	19.1	97	9.7	142	14.2
	spindle	10^3	358	35.8	156	15.6	80	8.0	406	40.6
	rod	10^3	192	19.2	128	12.8	67	6.7	613	61.3